

1973

Direct current flow through thin polymer films

Karl Arthur Sassaman
Lehigh University

Follow this and additional works at: <https://preserve.lehigh.edu/etd>



Part of the [Electrical and Computer Engineering Commons](#)

Recommended Citation

Sassaman, Karl Arthur, "Direct current flow through thin polymer films" (1973). *Theses and Dissertations*. 4174.
<https://preserve.lehigh.edu/etd/4174>

This Thesis is brought to you for free and open access by Lehigh Preserve. It has been accepted for inclusion in Theses and Dissertations by an authorized administrator of Lehigh Preserve. For more information, please contact preserve@lehigh.edu.

DIRECT CURRENT FLOW THROUGH THIN POLYMER FILMS

by

Karl Arthur Sassaman

A Thesis

Presented to the Graduate Committee

of Lehigh University

in Candidacy for the Degree of

Master of Science

in

The Department of Electrical Engineering

This thesis is accepted and approved in partial fulfillment of the requirements for the degree of Master of Science.

8/31/73

(date)

Frank H. Hilscher

Professor in Charge

A. K. Furheid

Chairman of Department

| TABLE OF CONTENTS | PAGE |
|--|------|
| TITLE PAGE | i |
| CERTIFICATE OF APPROVAL | ii |
| TABLE OF CONTENTS | iii |
| LIST OF TABLES | iv |
| LIST OF FIGURES | v |
| ABSTRACT | 1 |
| Part 1. INTRODUCTION | 2 |
| Part 2. SAMPLE PREPARATION AND EXPERIMENTAL PROCEDURE | 9 |
| 2.1 Sample Preparation | 9 |
| 2.2 Experimental Procedure | 13 |
| Part 3. EXPERIMENTAL RESULTS | 17 |
| 3.1 General Discussion | 17 |
| 3.2 Polystyrene | 21 |
| 3.3 CPE | 32 |
| 3.4 PEMA | 32 |
| 3.5 The Maleic Anhydride Copolymer | 40 |
| Part 4. SUMMARY | 47 |
| BIBLIOGRAPHY | 50 |
| VITA | 51 |

LIST OF TABLES

PAGE

| | | |
|----------|---|----|
| Table 1. | Range of resistivities | 18 |
| Table 2. | Experimental values of breakdown fields | 20 |
| Table 3. | Previously reported values of intrinsic breakdown fields . . | 20 |

LIST OF FIGURES**PAGE**

| | | |
|------------|---|----|
| Figure 1. | Sample structure | 10 |
| Figure 2. | Electrode geometry and spacing | 10 |
| Figure 3. | Circuit diagram used to obtain current-voltage data | 14 |
| Figure 4. | Shielded chamber used for obtaining current-voltage data | 15 |
| Figure 5. | Polystyrene on n type substrate | 22 |
| Figure 6. | Polystyrene on n type substrate | 23 |
| Figure 7. | Polystyrene on n type substrate | 24 |
| Figure 8. | Polystyrene on n type substrate | 25 |
| Figure 9. | Polystyrene on n type substrate | 26 |
| Figure 10. | Polystyrene on n type substrate | 27 |
| Figure 11. | Polystyrene on p type substrate | 28 |
| Figure 12. | Polystyrene on p type substrate | 29 |
| Figure 13. | CPE on p type substrate | 33 |
| Figure 14. | PEMA on p type substrate | 34 |
| Figure 15. | PEMA on p type substrate | 35 |
| Figure 16. | PEMA on n type substrate | 36 |
| Figure 17. | PEMA on n type substrate | 37 |
| Figure 18. | PEMA on p type substrate | 38 |
| Figure 19. | PEMA on p type substrate | 39 |
| Figure 20. | MA copolymer on p type substrate | 41 |
| Figure 21. | MA copolymer on p type substrate | 42 |
| Figure 22. | MA copolymer on n type substrate | 43 |
| Figure 23. | MA copolymer on n type substrate | 44 |

ABSTRACT

The d.c. current-voltage behavior of thin films (600^oÅ to 1500^oÅ) of four different polymers was observed. The polymers studied were polystyrene, chlorinated polyethylene, polyethylmethacrylate, and a copolymer of n-octadecyl-vinyl-ether and maleic anhydride. The films were solution deposited onto both p and n type silicon substrates. Aluminum electrodes were used to provide contact to the film. Voltages of both polarities were applied to the aluminum electrodes to obtain detailed current-voltage data.

The results for polystyrene and for chlorinated polyethylene films indicate space charge limited currents when silicon is used as the cathode. When aluminum is used as the cathode, space charge limitation is again observed, however with field dependence larger than that provided for in the simple theory.

For polyethylmethacrylate and the maleic anhydride copolymer, current flow was limited by field emission. For the maleic anhydride copolymer, the results agreed well with a theoretical prediction of internal field emission, i.e. with the Poole-Frenkel effect.

Part 1. INTRODUCTION

Dielectric materials have been used primarily for their insulating properties, however, all real dielectrics do in fact store charge and conduct current to some extent. Thus considerable interest has been displayed in the subjects of charge storage and current flow in dielectric materials. More recently, greater interest has been shown particularly in thin polymer films and their possible applications to electronic devices. For example, at the 1973 Electronics Components Conference in Washington, Seiki Haradi [1] described a process in which thin polyimide films were used, instead of silicon dioxide, as insulating layers in integrated circuits. According to Haradi, the use of thin polyimide layers eliminates failures caused by circuit openings in multilevel devices and also reduces the number of short circuits caused by pinholes. Use of polyimide films may thus increase the reliability and yield for these devices. Bui, Carchana, and Sanchez [2] have reported on experiments in which thin polymer films in MPS (metal-polymer-silicon) structures have been used to passivate dielectric films on silicon. Also, at the October 1972 meeting of the Electrochemical Society [3], considerable interest was expressed in the electret behavior of polymer films and of other dielectric materials. In fact, it has been

discovered that some thin polymer films exhibit both electret and piezo-electric effects and thus can be used as transducers [3]. Although much interest has been shown in thin polymer films and their uses, very little is known about the exact nature of their charge storage and current flow mechanisms.

It is known that charge is stored in thin polymer films [2], however much work remains to be done to find out what kind of charge is stored (positive or negative, electronic or ionic), the location of the stored charge (near the interface or in the bulk of the material), and how the charge is stored (shallow traps, deep traps, etc.). As is true for all real dielectric materials, current flow through polymer films has been observed and some data on this subject has been published [4-9]. For most materials, however, very little detailed d.c. data is available. Furthermore, in the few cases where detailed data have been reported, the samples used were of bulk material, probably containing many defects which may have seriously affected the accuracy of the data. Also, most of the data is reported incompletely with frequent omissions of information regarding the size of the electrode areas and of the thicknesses of the films used. There exist a number of theories [5,10], for possible current flow mechanisms in thin polymer films, but it is

not always clear which of the mechanisms applies in specific cases.

This thesis is a presentation of d.c. current-voltage data experimentally obtained from samples of thin films of four different polymers. Tables of resistivities (at specific applied electric fields) and of measured breakdown fields are also given for these polymers. An attempt is made to see which, if any, of the possible current flow mechanisms apply to our polymers.

Thin polymer films are studied because they are most likely to be defect free, at least in those areas of the film which were used for obtaining the data. Any gross structural defects in the films of the thicknesses used here (600\AA to 1500\AA) can readily be observed by visual inspection under a microscope. By avoiding areas of the film which contain visible defects, we were reasonably sure that the data obtained most nearly represents the actual current-voltage behavior of the polymer material. Also, since defects in dielectric films tend to cause breakdown to occur at lower fields [11], the breakdown fields reported here more closely represent the actual breakdown fields of the material than those reported on bulk polymer samples.

Many possible current flow mechanisms for dielectrics can be found in the literature. For instance, Sze [12] lists the following:

| Process | Expression |
|---------------------------------|---|
| 1. Schottky emission | $J = A^* T^2 \exp[-q(\phi_b - (qE/4\pi\epsilon_i)^{1/2})/kT]$ |
| 2. Poole-Frenkel | $J = E \exp[-q(\phi_b - (qE/\pi\epsilon_i)^{1/2})/kT]$ |
| 3. Tunnel or field emission | $J = E^2 \exp[4(2m^*)^{1/2}(q\phi_b)^{3/2}/3q\hbar E]$ |
| 4. Space charge limited current | $J = 8\epsilon\mu V^2/9d^3$ |
| 5. Ohmic conduction | $J = E \exp(-\Delta\epsilon_e/kT)$ |
| 6. Ionic conduction | $J = (E/T) \exp(-\Delta\epsilon_{ai}/kT)$ |

A^* = effective Richardson constant
 T = temperature in degrees Kelvin
 q = electronic charge
 ϕ_b = barrier height
 E = electric field
 ϵ_i = insulator dynamic permittivity
 k = Boltzmann's constant
 m^* = effective mass
 \hbar = Planck's constant divided by 2π
 μ = mobility
 V = applied voltage
 d = insulator thickness
 $\Delta\epsilon_e$ = activation energy of electrons
 $\Delta\epsilon_{ai}$ = activation energy of ions

The most likely of these are briefly reviewed here.

One frequently suggested mechanism is space charge limited current flow [9,10]. Lampert [10] compares space charge limited current flow in insulators to that in a vacuum. The equation suggested by Lampert for a perfect insulator is:

$$J \approx \epsilon \mu V^2 / L^3 \quad (1)$$

where ϵ is the dielectric constant, μ is the mobility, and L is the electrode spacing (in the case of a vacuum dielectric) or the film thickness (in the case of a dielectric film, where the electrodes make contact with the film). Equation (1) can be written in terms of the electric field with the following result:

$$J \approx (\epsilon \mu / L) E^2. \quad (2)$$

Taking the logarithm of both sides of equation (2) yields:

$$\log(J) \approx K + 2 \log(E) \quad (3)$$

where K is a constant (for the specific geometry).

Equation (3) indicates that a plot of $\log(J)$ vs. $\log(E)$ will be linear with a slope of approximately 2 if the current is space charge limited. This result is expected for a pure insulator without traps. Theoretical calculations of space charge limited currents in insulators containing traps show that a linear $\log(J)$ vs. $\log(E)$ plot will still result, in this case with a slope of 2 or greater.

In addition to space charge limited current flow,

there are two other frequently considered mechanisms, which involve the excitation of electrons over potential barriers. One of these, Schottky emission, is concerned with potential barriers at the metal-insulator interface, whereas, the other, the Poole-Frenkel effect, is concerned with potential barriers at trap sites within the insulator. Although theoretical current-voltage relationships are similar for these two cases, one can distinguish between them by a detailed analysis of the results, as discussed by Jonscher [5].

Other possible current flow mechanisms, which are not considered here, are ohmic conduction, diffusion, and ionic conduction. Ohmic conduction was not observed in this investigation and if it exists for these materials, it would probably take place at fields much lower than 10^5 V/cm. Diffusion currents are not considered because of the very high electric fields used in this study. Ionic conductivity, which yields a direct proportionality between J and E, was not considered since such a relationship was not found.

The data obtained in this investigation indicated that the primary mechanisms responsible for this observed current-voltage behavior are space charge limited current flow, which yields a linear $\log(J)$ vs. $\log(E)$ relationship, and the Poole-Frenkel effect which yields a linear $\log(J/E)$

vs. E^{\dagger} relationship.

Part 2. SAMPLE PREPARATION AND EXPERIMENTAL PROCEDURE

2.1 Sample Preparation

Figure (1) shows the physical structure of the samples used for investigating the current-voltage behavior of the thin polymer films. Figure (2) is a top view of the sample showing the approximate spacing and positioning of the aluminum electrodes. Two sizes of electrodes were used, 10 mil diameter circles and 20 mil diameter circles. The distance [a] is the nearest edge spacing which is about 5 mils for the 10 mil circles and 10 mils for the 20 mil circles.

Silicon slices were used as substrates because they were available with a highly polished flat surface, and because such substrates had been used in previous studies to determine the extent of electronic charge storage in thin polymer films by the means of capacitance-voltage measurements. Both p type and n type silicon substrates were used to determine whether the conductivity type of the substrate had any effect on the current-voltage behavior of the polymer films. The silicon slices were provided with a gold backing to insure ohmic contact to the silicon. A vacuum system and stainless steel masks containing 10 mil diameter and 20 mil diameter circles were available.

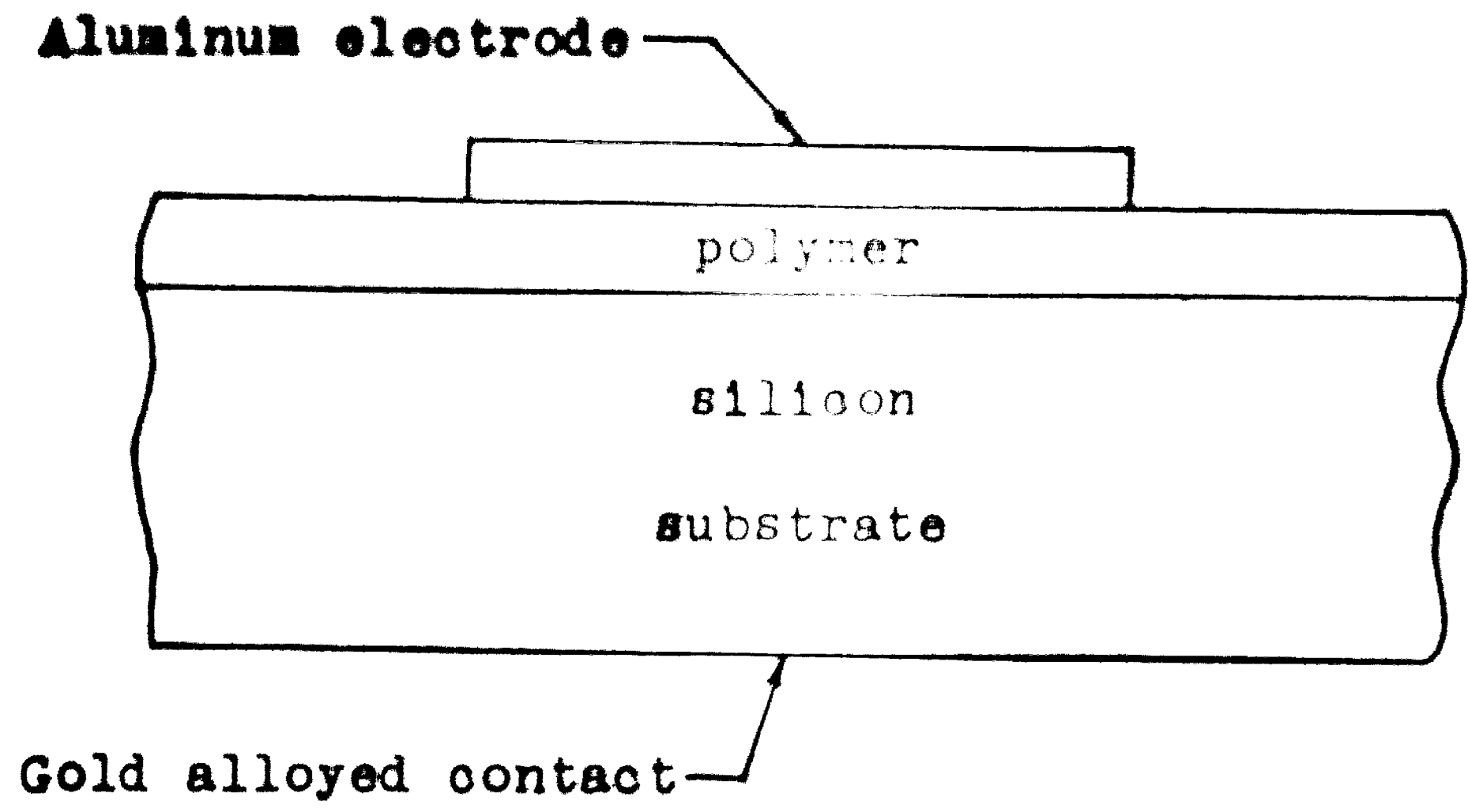


Figure 1. Sample structure.

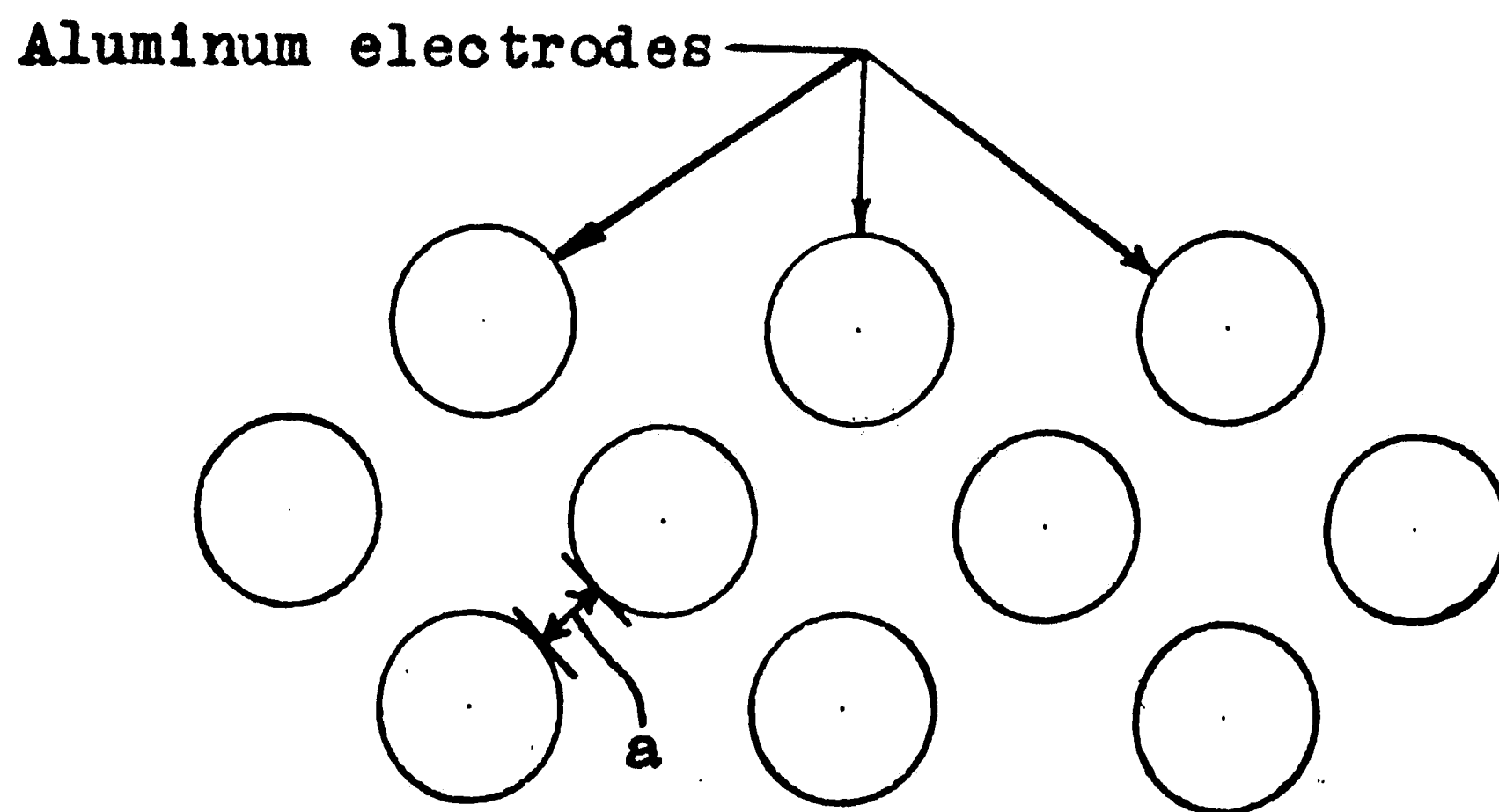


Figure 2. Electrode geometry and spacing.

and were used to vacuum deposit the aluminum electrodes onto the films. Aluminum was used because it was readily available, it was convenient to use in the vacuum evaporation process, it provided a good electrical contact, and it adhered well to the polymer films. Thin films of the polymers on the order of 600Å to 1500Å were used because defects in films this thin can easily be detected under a microscope. Areas free of visual defects were believed to closely represent the pure defect free polymer material.

To prepare the silicon slices for use as substrates, gold was first evaporated onto the backs of the slices and then alloyed into the slices. Before the polymer films were applied, the slices were cleaned using the following chemical steps:

1. immersion in hot trichloroethylene
2. immersion in hot acetone
3. immersion in hot alcohol
4. rinse with de-ionized H₂O
5. immerse in hot H₂SO₄ + H₂O
6. rinse with de-ionized H₂O
7. dip in solution of 1 part HF to 9 parts H₂O
8. rinse several times in de-ionized H₂O

The HF dip (step 7) was done immediately before application of the polymer film in order to reduce the amount of silicon dioxide formation on the silicon surface. Solutions of the polymers were dropped onto the substrates with a dropper and the substrates were

then spun, using a vacuum chuck, at approximately 10,000 rpm to produce the films. The solutions used were 5% to 10% polymer by weight in solvent. The polymers used were polystyrene, chlorinated polyethylene (CPE), polyethylmethacrylate (PEMA), and a copolymer of n-octadecyl vinyl ether and maleic anhydride (MA). Xylene was used as the solvent for polystyrene and CPE. Benzene was used as the solvent for PEMA and tetrahydrofuran was used for the MA copolymer. Different film thicknesses were obtained by varying the spinner speed and/or amount of polymer in solution. Film thicknesses were determined by comparing the color of the film with a color chart prepared for SiO_2 ($n=1.46$), and by the use of a Tolansky multiple beam interferometer.

After the films were formed, they were first inspected to see if the film was of constant thickness over most of the substrate. Next they were inspected under a microscope for gross defects such as pinholes and radial streaks. In order for a sample to be usable, it had to have defect free areas large enough to contain the 10 mil or 20 mil electrodes.

If a sample was found to be unsatisfactory, the film was stripped, the substrate was cleaned, and a new

film was made. The last step in making the samples was the vacuum deposition of the aluminum electrodes onto the polymer films. Introduction of the samples into the vacuum chamber for the evaporation step also had the effect of purging the films of moisture. The importance of this is explained later.

2.2 Experimental Procedure

Figure (3) shows the circuit diagram of the measuring system used to obtain the current-voltage data.

Figure (4) shows the shielded chamber used to reduce external electrical noise while taking data. During the process of gathering data from the initial slices, it was found that moisture and light affected the current-voltage characteristics. Thus the chamber was sealed using a pliable silicone cement to keep out moisture and light and a moisture absorbing agent (calcium sulfate) was placed inside the chamber.

Contact was made to the back of the sample by placing it on the gold-plated copper block which was connected to ground. Contact to the aluminum electrodes was made with a spring-loaded gold-plated probe mounted on a micromanipulator to facilitate positioning. A

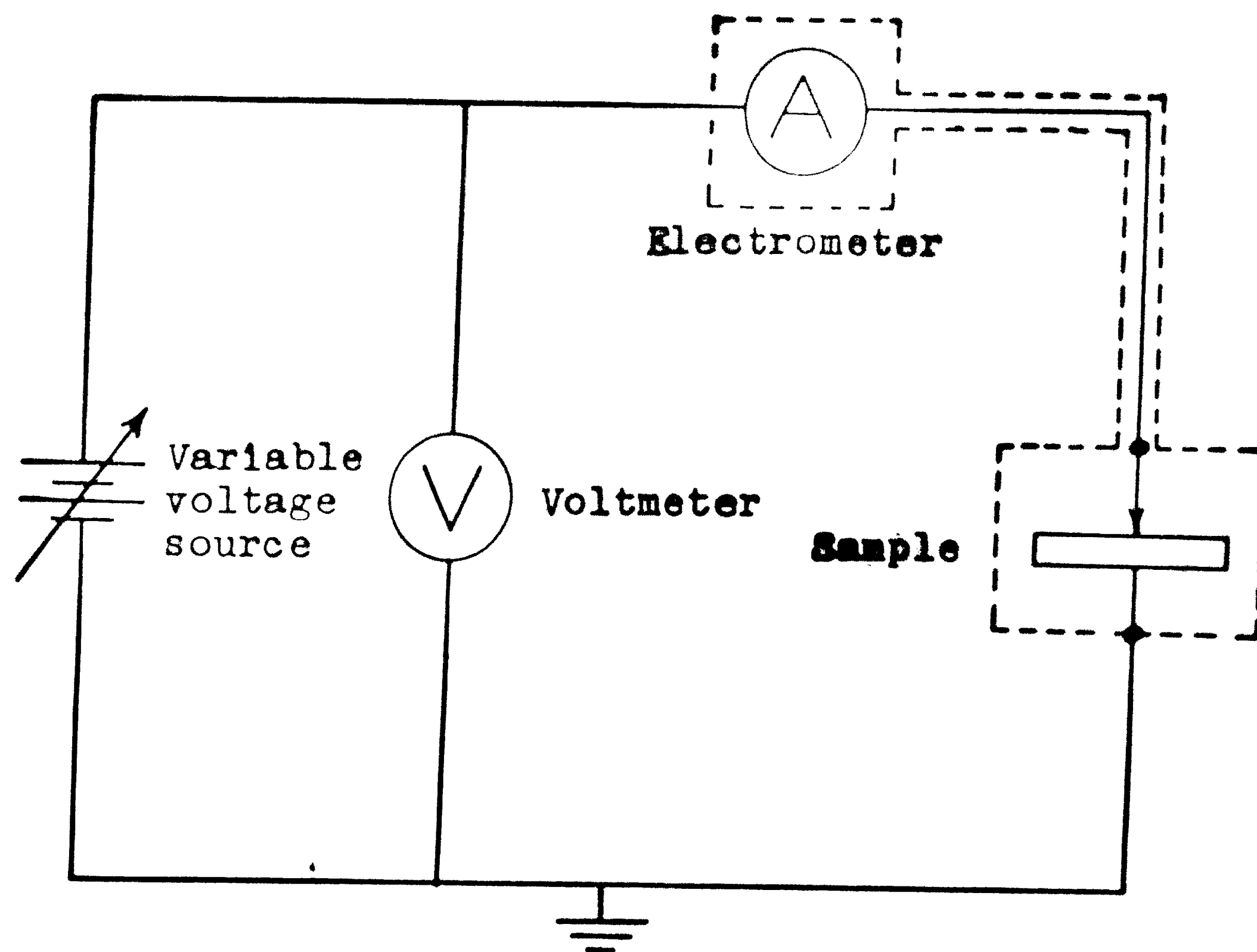


Figure 3. Circuit diagram used to obtain current-voltage data.

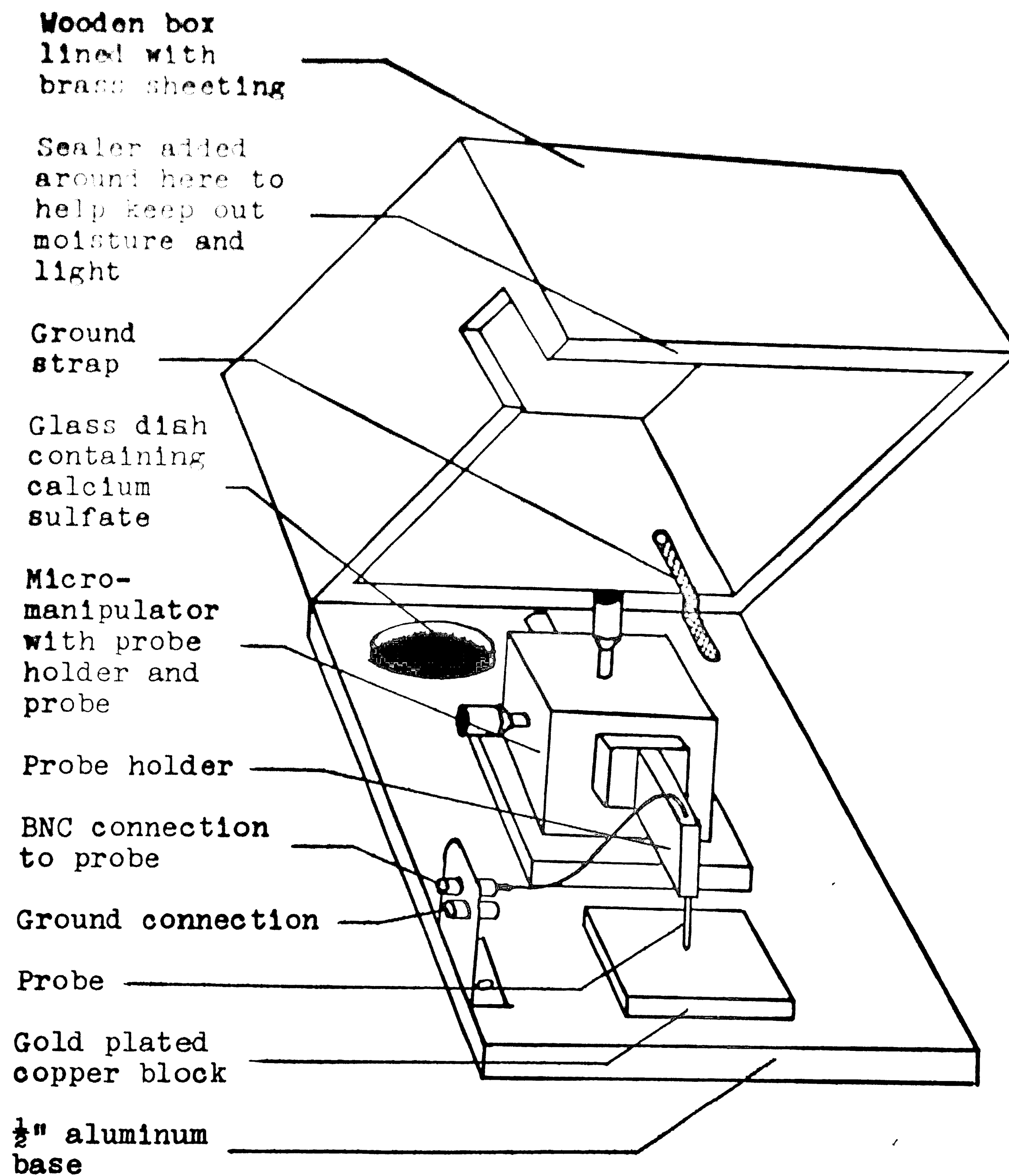


Figure 4. Shielded chamber used for obtaining current-voltage data.

Power design model 5015 power supply was used as the voltage source. A PAR model 135 battery operated electrometer was used to measure the current and a Heathkit model IM-104 multimeter was used to measure voltage. The electrometer was used in the feedback mode so that the voltage drop across the instrument was never more than one millivolt. Thus the voltage across the power supply was essentially equal to the voltage across the sample. This made it easier to measure the voltage, since one of the leads to the sample was shielded.

Prior to making detailed current-voltage measurements, several measurements were made on each sample to determine the breakdown voltages of the films. Current-voltage measurements were then initiated by applying the highest voltage which could be used without breakdown, and then data was recorded for successively decreasing voltages. Separate sets of data were recorded for positive and negative voltages applied to the aluminum electrodes.

Since charge storage in these films is a relatively slow process, it was necessary to wait several minutes at each voltage setting until a steady state current could be measured.

Part 3. EXPERIMENTAL RESULTS

3.1. General Discussion

In this part, some observations common to all of the polymers are discussed first. This general discussion is followed by a detailed analysis of the data for each polymer.

After completion of the current-voltage measurements for each sample, moisture was introduced to the sample by breathing on it. In every case, this had the effect of increasing the current by several orders of magnitude, and is illustrated in part 3.2 for polystyrene. It was also observed that light shining on the films had the effect of increasing the current somewhat, typically by a factor of 2.

Table 1 contains ranges of values for resistivities at 10^6 V/cm and 10^5 V/cm. Since current flow through insulators is nonohmic, it should be kept in mind that these values are valid only at the corresponding applied electric field and are meaningless at other fields. A number of resistivity values were calculated, from the plots for each polymer, therefore the highest and lowest of these values are recorded to indicate the range of resistivities for each polymer. In most cases, the curves

| Polymer | Range of resistivities | |
|--------------|-----------------------------|------------------------|
| | @ 1×10^6 V/cm | @ 1×10^5 V/cm |
| Polystyrene | 8.7×10^{12} ohm-cm | 10^{13} ohm-cm |
| | 1.0×10^{16} ohm-cm | 10^{20} ohm-cm |
| CPE | 1.1×10^{11} ohm-cm | 10^{11} ohm-cm |
| | 5.7×10^{11} ohm-cm | 10^{15} ohm-cm |
| PEMA | 4.8×10^{13} ohm-cm | 10^{14} ohm-cm |
| | 3.8×10^{17} ohm-cm | 10^{21} ohm-cm |
| MA copolymer | 2.2×10^{13} ohm-cm | 10^{15} ohm-cm |
| | 6.7×10^{13} ohm-cm | 10^{17} ohm-cm |

Table 1. Ranges of resistivities.

had to be extrapolated in order to calculate values at 10^5 V/cm, thus these are only approximate values.

Table 2 lists the breakdown fields measured for each of the polymers. It should be emphasized here that these values are lower bounds, and that the actual breakdown fields may be somewhat higher. The breakdown data presented here agrees reasonably well with previously published intrinsic breakdown field data (see table 3), which suggests that the polymer films used in this study closely represent the intrinsic polymer material.

It should again be noted that two sizes of electrodes were used. Initially, 10 mil diameter circles were used, but later 20 mil diameter circles were used so that the current could more easily be measured, particularly for smaller applied voltages. The size of the electrode used is indicated for every plot and is expressed as the area of the electrode, A (10 mil diameter, $A=5 \times 10^{-4} \text{cm}^2$; 20 mil diameter, $A=2 \times 10^{-3} \text{cm}^2$). The thickness of the film, denoted by X_0 , is also given for every plot and is expressed in units of Angstroms. Unless otherwise noted, (+) symbols on the plots represent positive voltages applied to the aluminum electrode and (•) symbols represent negative voltages applied to the aluminum electrodes. J denotes the current density in units of $[\text{A}/\text{cm}^2]$, and E denotes the electric field in units of $[\text{V}/\text{cm}]$.

| Polymer | Breakdown field |
|--------------|-------------------------------------|
| Polystyrene | $\geq 3.7 \times 10^6 \text{ V/cm}$ |
| CPE | $\geq 3.5 \times 10^6 \text{ V/cm}$ |
| PEMA | $\geq 6.7 \times 10^6 \text{ V/cm}$ |
| MA copolymer | $\geq 2.0 \times 10^6 \text{ V/cm}$ |

Table 2. Experimental values of the breakdown fields.

| Polymer | Breakdown field |
|-------------|--------------------------------|
| Polystyrene | $6 \times 10^6 \text{ V/cm}$ |
| CPE | $6.5 \times 10^6 \text{ V/cm}$ |
| PMMA* | $10 \times 10^6 \text{ V/cm}$ |

Table 3. Previously reported values of intrinsic breakdown fields [13].

* Note that the breakdown field for PEMA is being compared with the intrinsic breakdown field for PMMA (polymethylmethacrylate), however, since these two polymers are similar, it is felt that such a comparison is justified.

Generally, data are illustrated on both a space charge limited plot ($\log(J)$ vs. $\log(E)$) and on a field emission limited plot ($\log(J/E)$ vs. $E^{1/2}$).

3.2 Polystyrene

The data for polystyrene are summarized in figures 5-12. Figures 5 and 6 illustrate data from samples of polystyrene which had been exposed to moisture. By comparing figures 5 and 6 with the other data for polystyrene, one can see that moisture not only increases the amount of current flow, but also changes the mechanism for current flow as well. In fact, in the curve for the positive applied voltages in figure 5 the slope is 1, indicating ohmic current flow in this particular case, while the slope of the curve for the negative applied voltages is 1.7, which suggests a different current flow mechanism than for positive voltages. In either case, one can see that moisture on or within the sample has a significant effect on the current flow. Figures 5 and 6 are the only data shown for a moist film, all of the remaining data for polystyrene and also for the other three polymers in the later subsections are shown for "dry" films.

The curves in figures 7, 9 and 11, representing space charge limited graphs for three polystyrene samples,

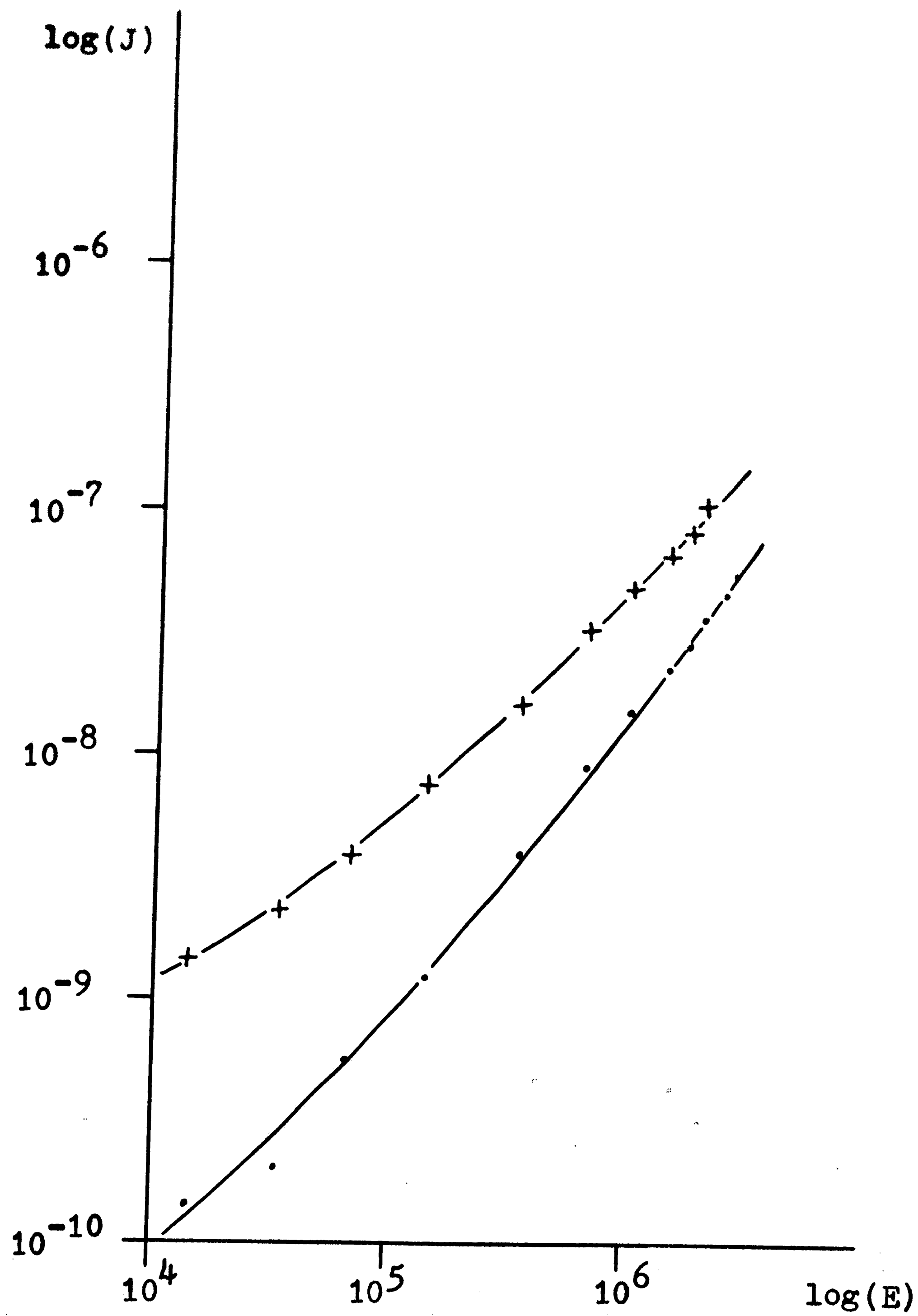


Figure 5. Polystyrene on n type substrate;

$X_0 = 1500\text{\AA}; A = 5 \times 10^{-4} \text{cm}^2.$

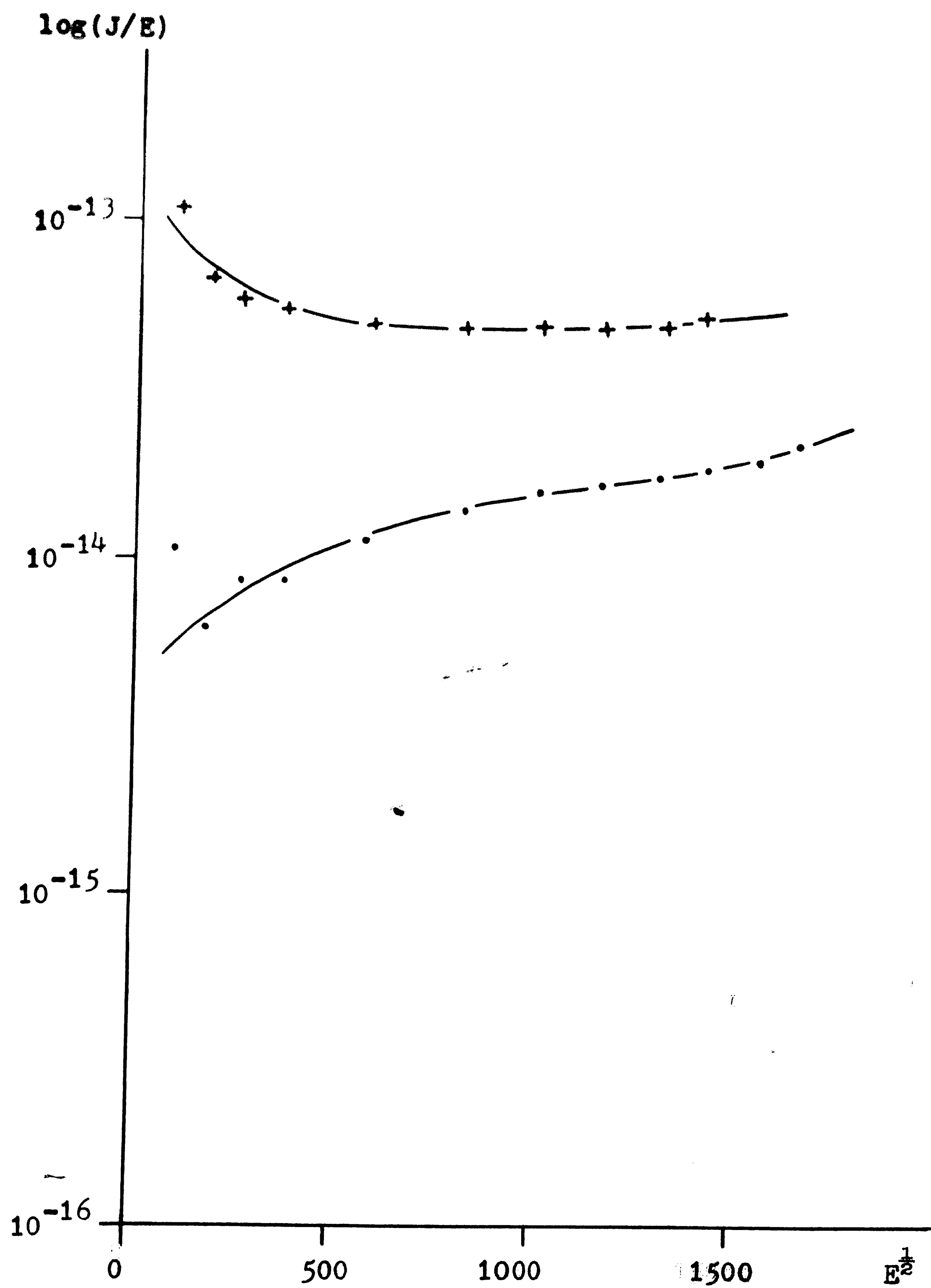


Figure 6. Polystyrene on n type substrate;
 $X_0 = 1500 \text{ \AA}$; $A = 5 \times 10^{-4} \text{ cm}^2$.

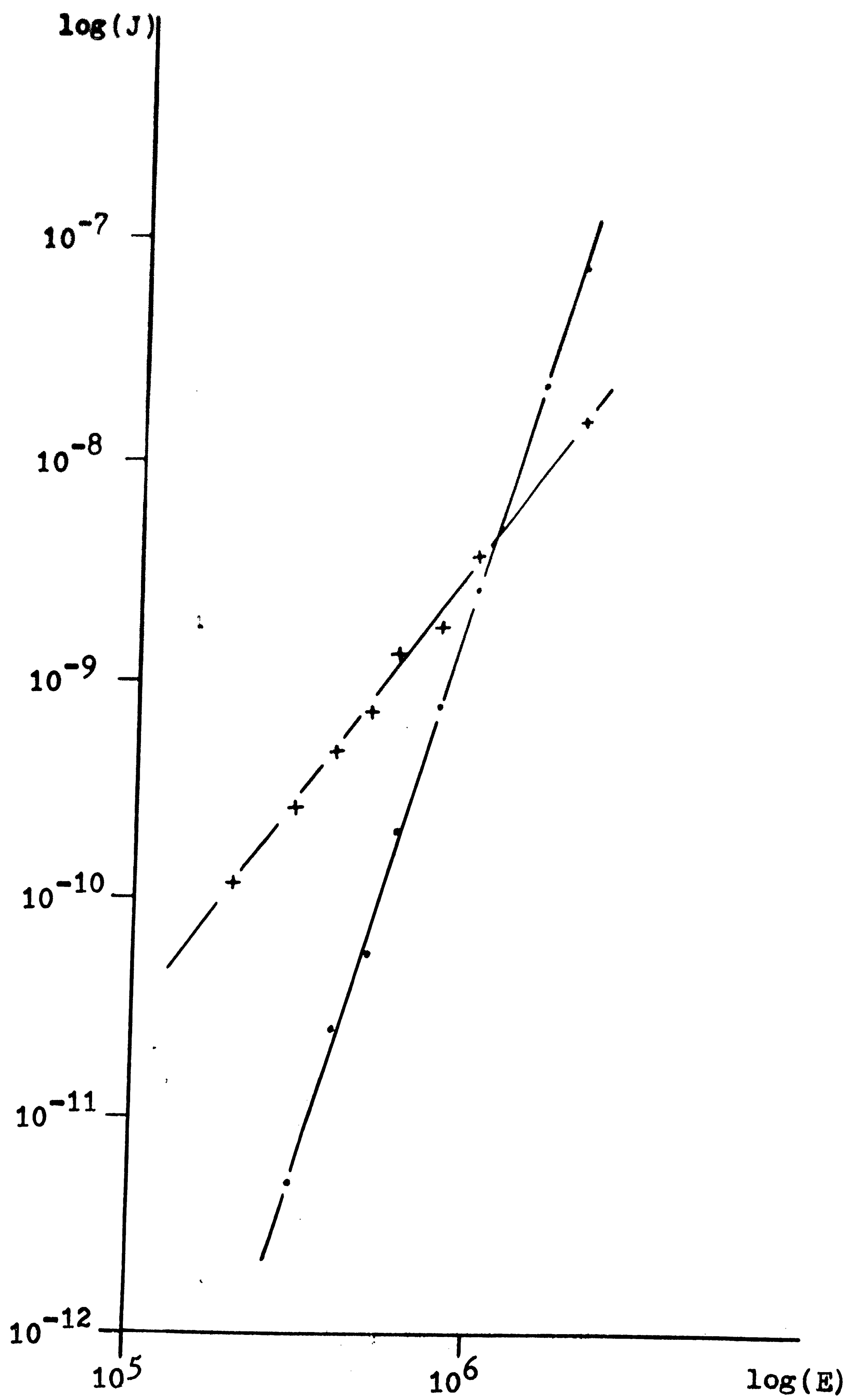


Figure 7. Polystyrene on n type substrate;
 $X_0 = 1000 \text{ \AA}$; $A = 2 \times 10^{-3} \text{ cm}^2$

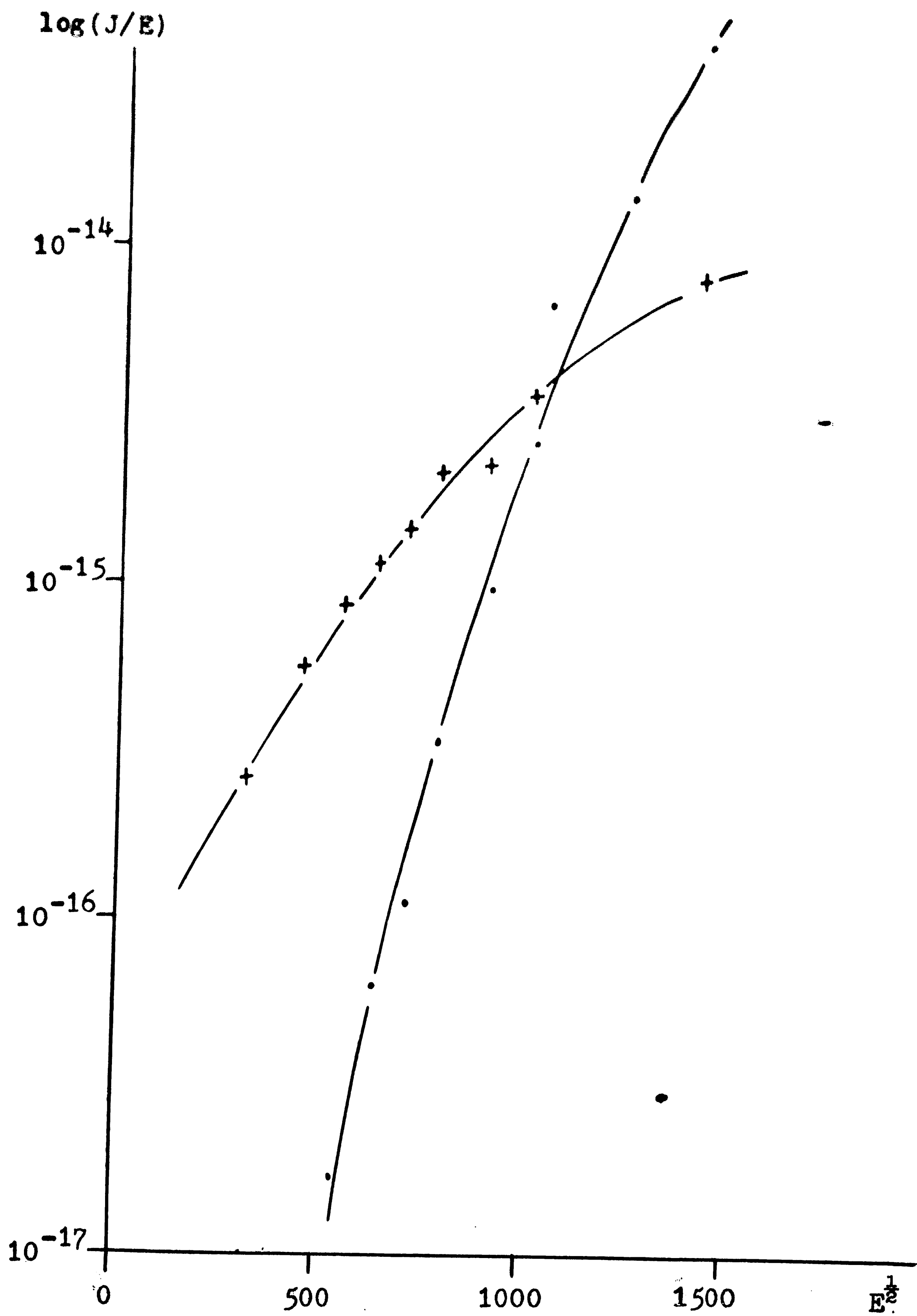


Figure 8. Polystyrene on n type substrate;

$X_0 = 1000 \text{ \AA}; A = 2 \times 10^{-3} \text{ cm}^2.$

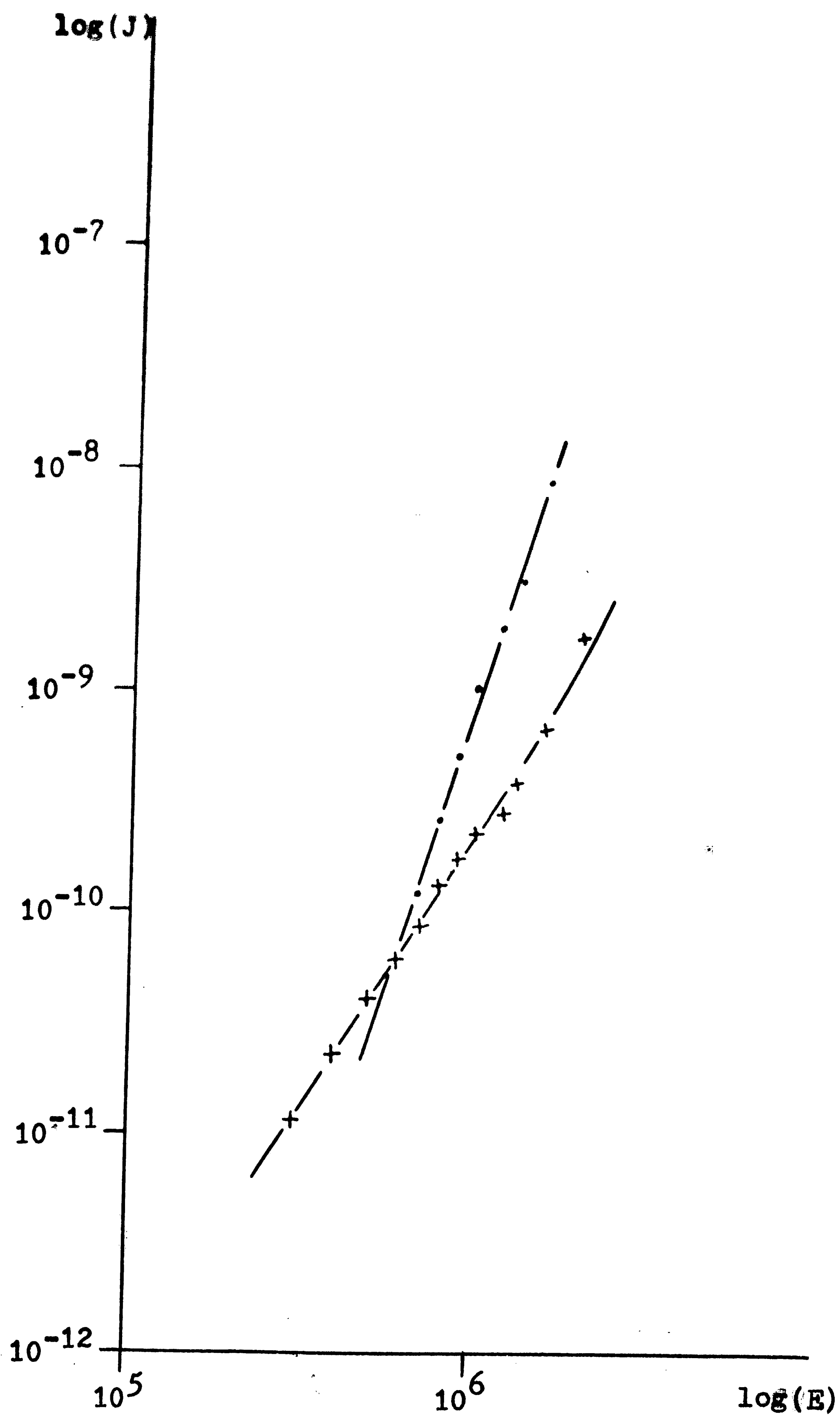


Figure 9. Polystyrene on n type substrate;
 $X_0 = 1000\text{\AA}$; $A = 2 \times 10^{-3} \text{cm}^2$.

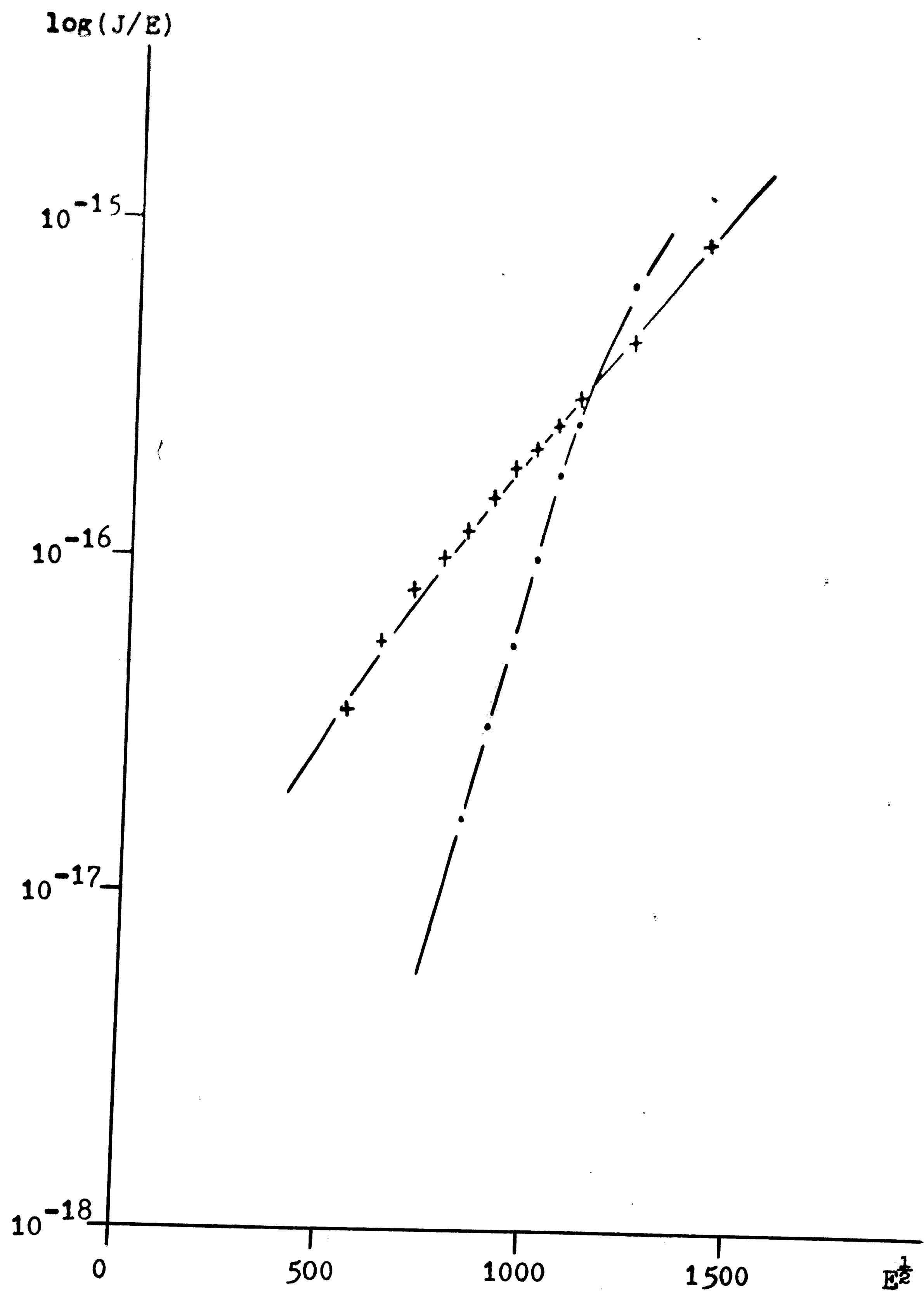


Figure 10. Polystyrene on ntype substrate;

$X_0 = 1000 \text{ \AA}; A = 2 \times 10^{-3} \text{ cm}^2.$

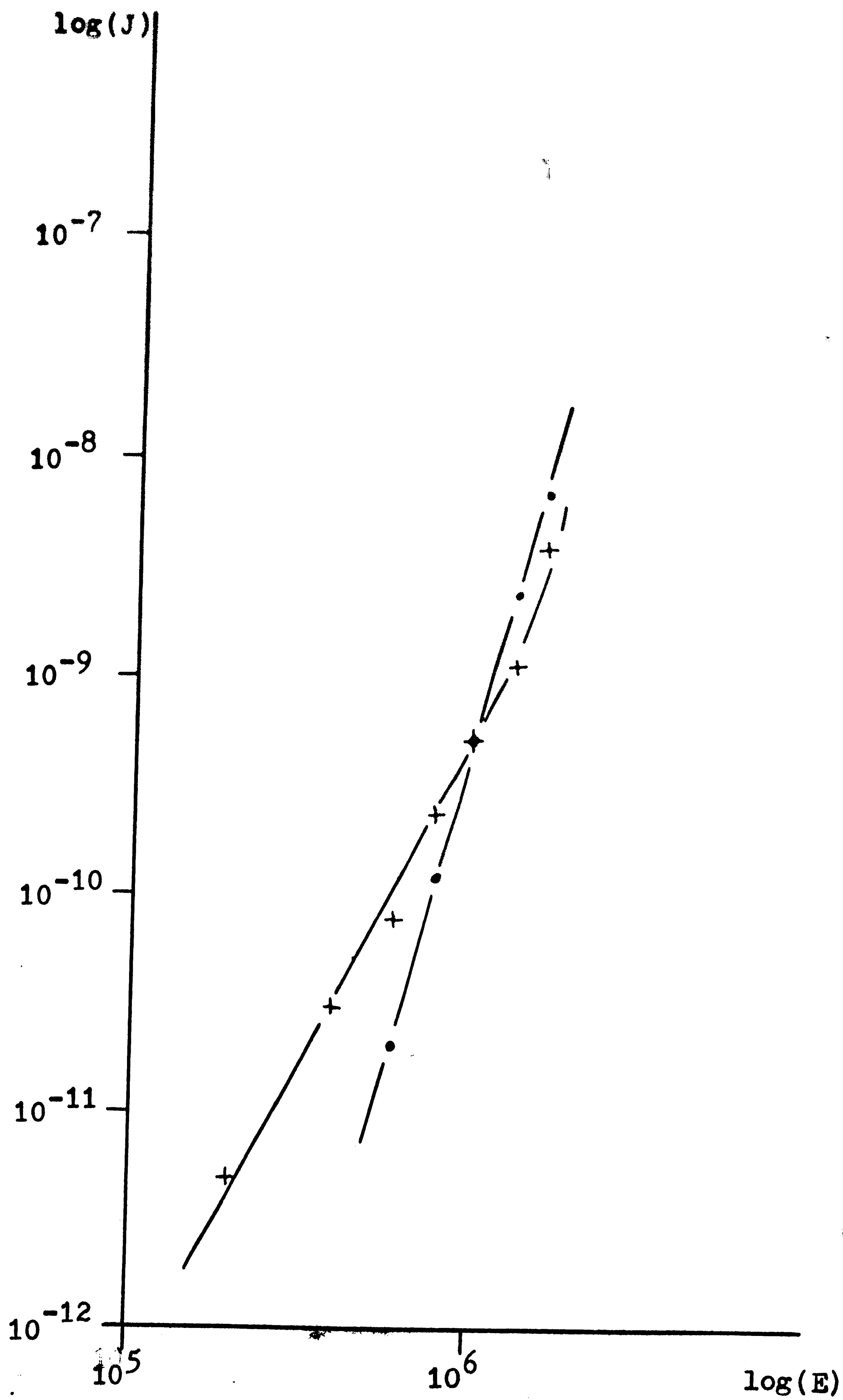


Figure 11. Polystyrene on p type substrate;

$X_0 = 1000\text{\AA}; A = 2 \times 10^{-3} \text{cm}^2.$

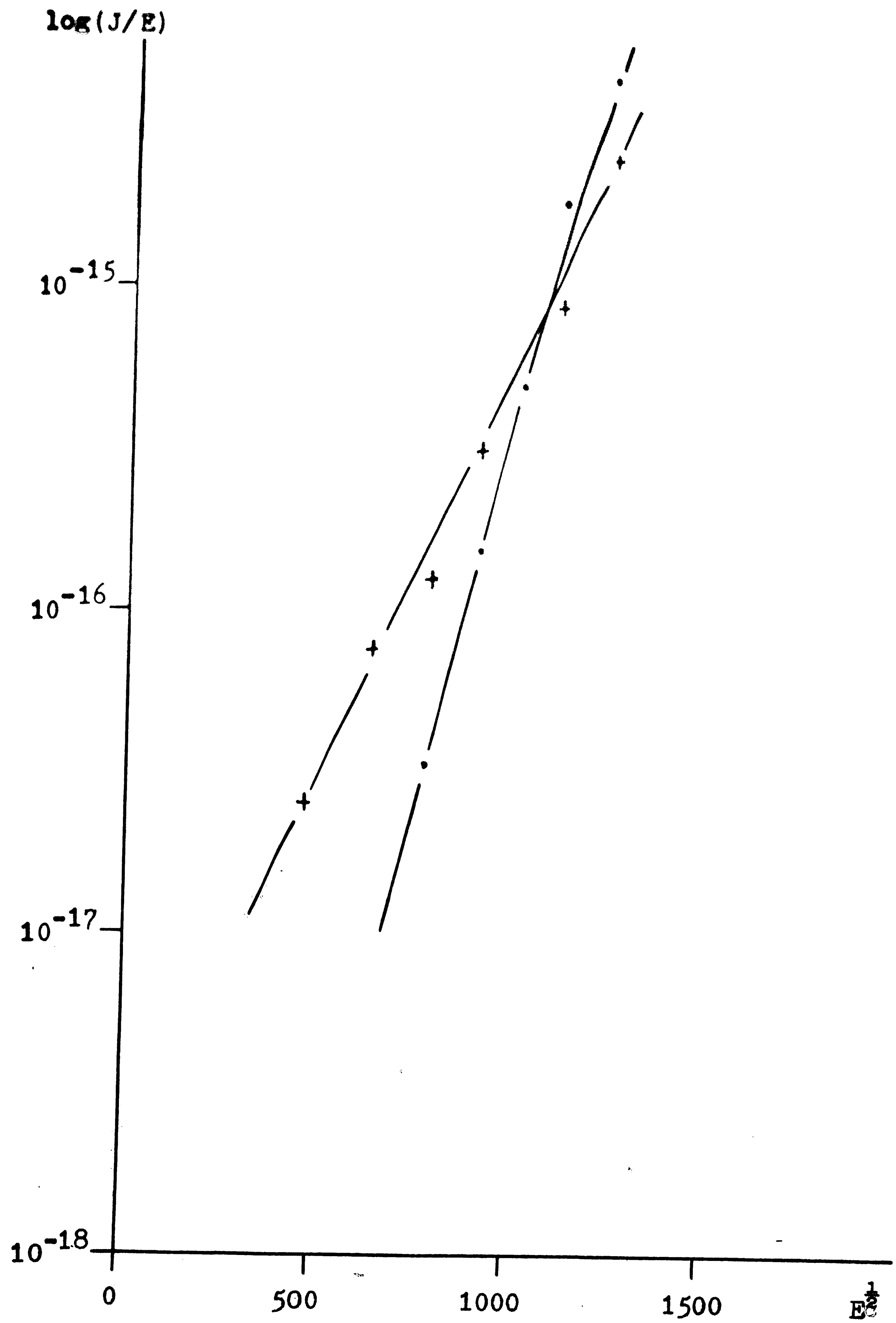


Figure 12. Polystyrene on p type substrate;

$X_0 = 1000 \text{ \AA}; A = 2 \times 10^{-3} \text{ cm}^2.$

indicate a difference in slope for positive and negative applied voltages. For positive applied voltages, the slope is approximately 2 in each case, except in figure 11 where it is approximately 3, which is the result expected for space charge limited current in either a trap free insulator or in an insulator containing a uniform distribution of shallow traps. The slope for negative applied voltages is approximately 5, which possibly suggests another current flow mechanism. Since the material is the same for both polarities (i.e. the trap configuration is the same), the difference between the positive and negative voltage data is quite possibly caused by the difference in electrode work functions (positive voltage is applied to the aluminum electrode in one case, and to the silicon in the other case).

Lampert [10] suggests the following equation for space charge limited current flow in an insulator with traps:

$$J \approx \epsilon \mu \theta E^2 / L$$

where θ is a function of trap occupancy and can vary with the applied electric field. If for high fields θ is proportional to E^3 , then a space charge limited plot with a slope of 5 could result, which suggests that the current flow for the negative voltages may also be space charge limited.

Figure 7 illustrates a straight line space charge limited plot for polystyrene while figure 8 exhibits a non-linear field emission plot for the same data. This data suggests that the current flow may be space charge limited for polystyrene. In this case, the current flow seems to be greater in magnitude, for positive applied voltages, than that illustrated in figures 9 and 11. It is not clear what causes this difference in magnitude since the material is believed to be essentially the same in all three cases.

The data in figure 9, which is for a sample with an n type substrate, bears much similarity to the data illustrated in figure 11, which is for a sample with a p type substrate, showing that the conductivity type of the substrate has little effect on the current flow in polystyrene.

Despite the straight line behavior of the curves shown on the space charge limited graphs (figure 9 and 11) it is not possible to unequivocally consider the actual current to be space charged limited, since when the same data is plotted on a field emission graph (figures 10 and 12), appreciable straight line segments also result. Thus, it is not clear which current mechanism applies, and additional data would be required

to resolve this problem, for example by measuring current as a function of insulator thickness.

3.3 CPE

The data for CPE is represented in figure 13. A field emission limited current plot of this data was also made, but it was clearly not linear and therefore it is not included. Thus the Poole-Frenkel effect does not apply for this case and some form of space charge limitation must be considered.

The data for the positive applied voltages indicate a slope of 2, which is the result expected for space charge limited current flow in either a trap free insulator or one which contains a uniform concentration of shallow traps. On the other hand however, a slope of 5 is indicated by the data for negative voltages. This suggests that a different mechanism for current flow takes place when negative voltages are applied to the aluminum electrode, perhaps space charge limited current flow in an insulator with traps as discussed previously for polystyrene in 3.2.

3.4 PEMA

The data for PEMA is summarized in figures 14-19. This data again exhibits a difference between positive

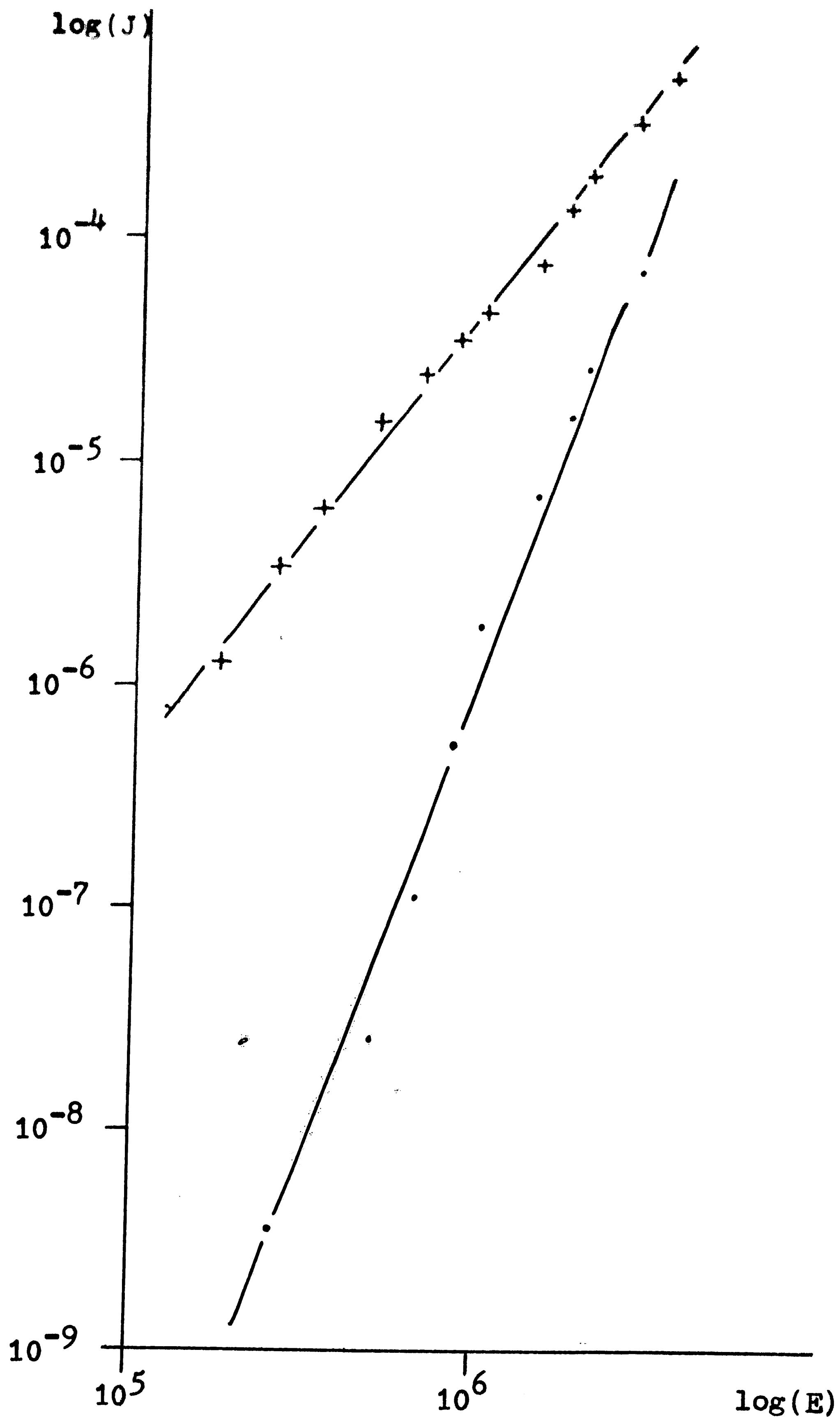


Figure 13. CPE on p type substrate;
 $X_0 = 600\text{\AA}$; $A = 2 \times 10^{-3} \text{cm}^2$.

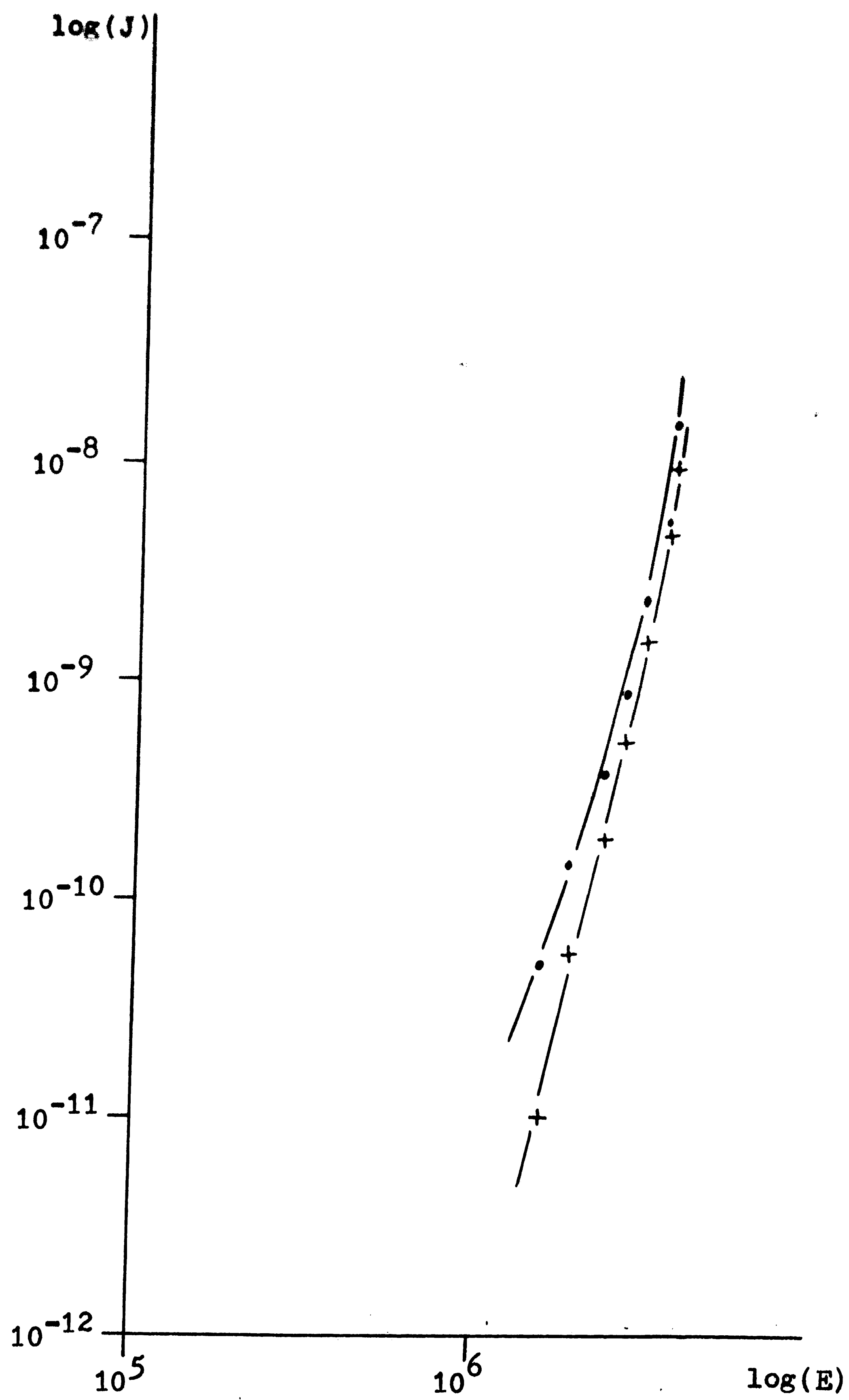


Figure 14. PEMA on p type substrate;
 $X_0 = 1300\text{\AA}$; $A = 2 \times 10^{-3} \text{cm}^2$.

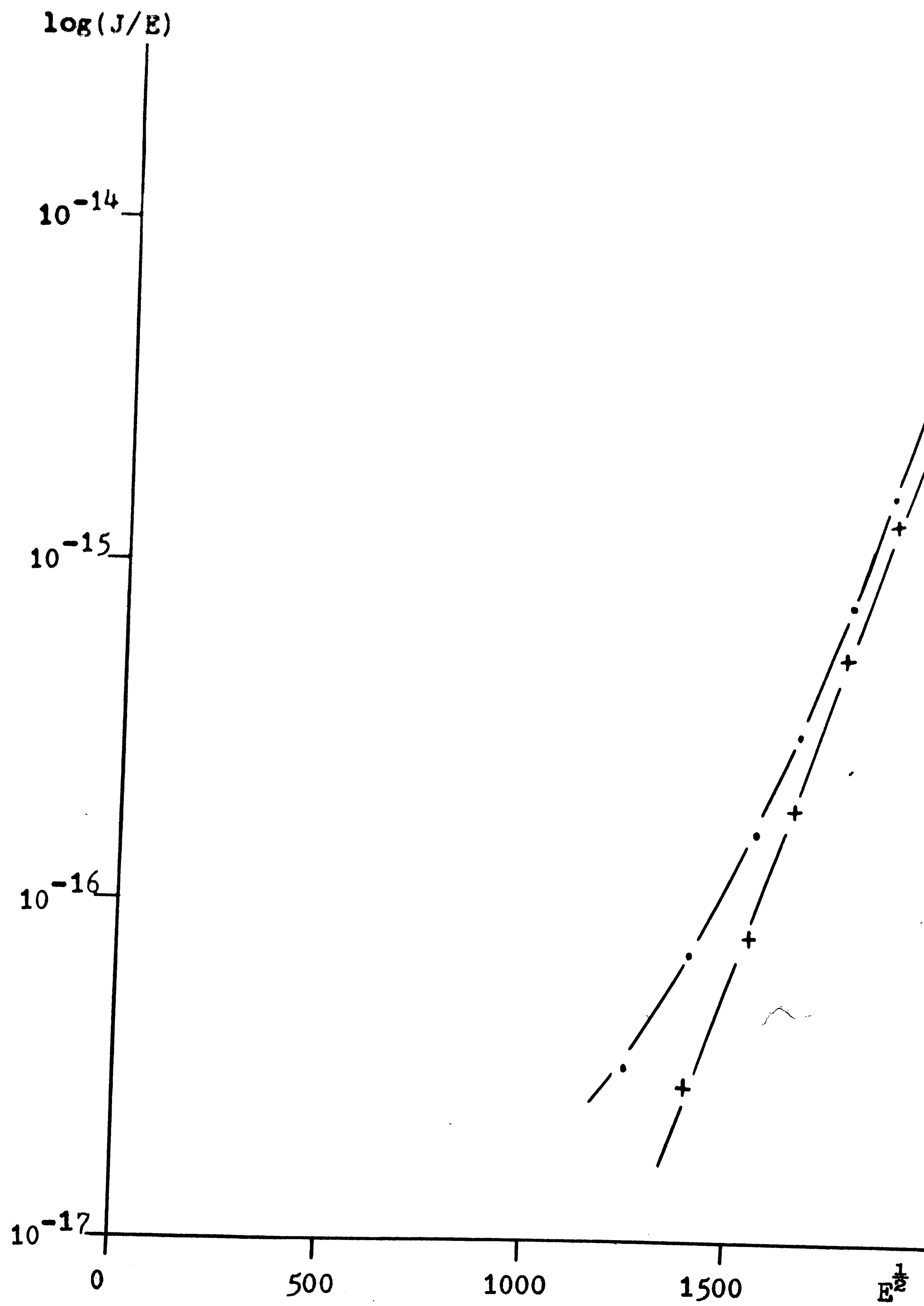


Figure 15. PEMA on p type substrate;
 $X_0=1300\text{\AA}$; $A=2 \times 10^{-3} \text{cm}^2$.

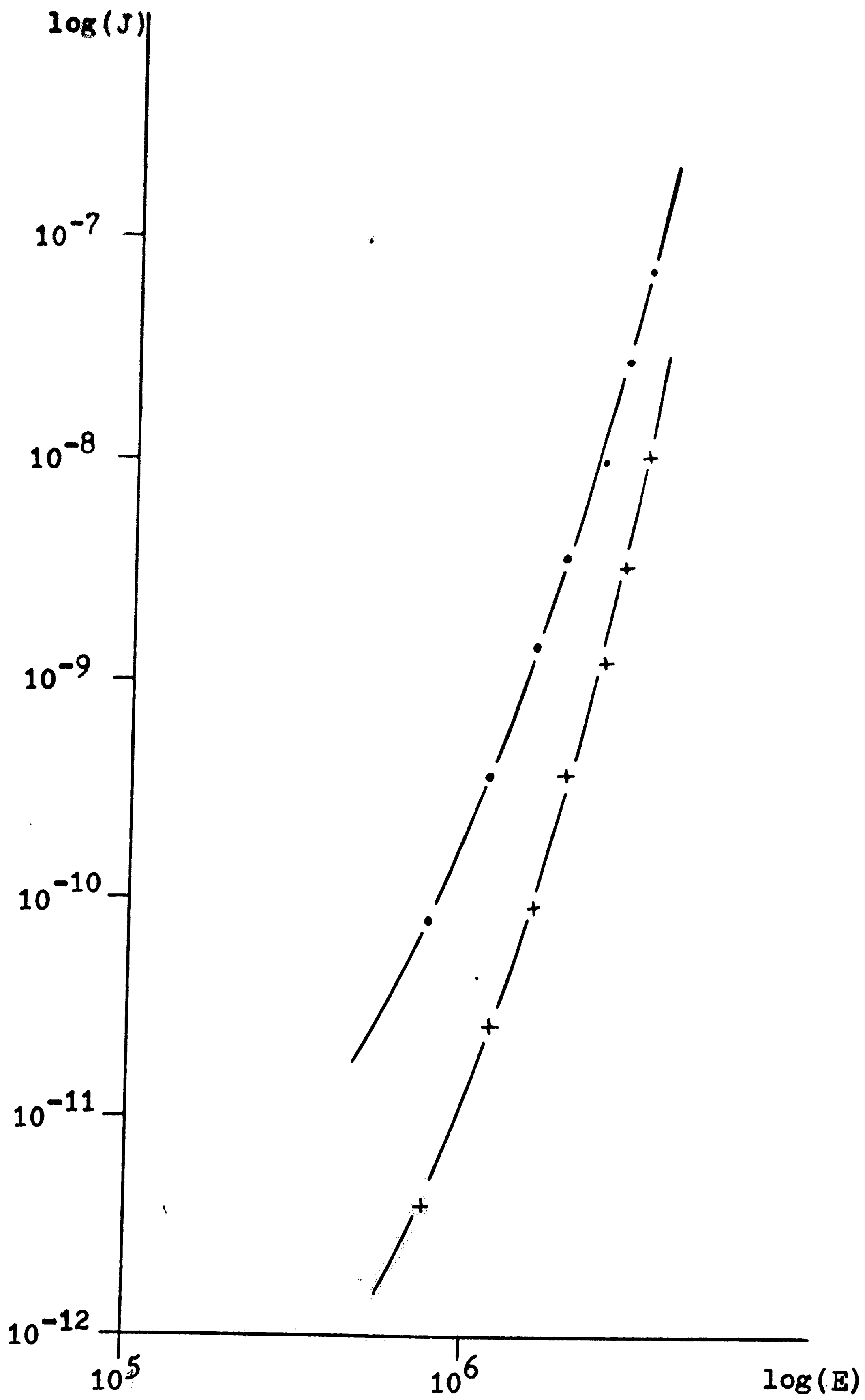


Figure 16. PEMA on n type substrate;

$X_0 = 1300\text{\AA}; A = 2 \times 10^{-3} \text{cm}^2.$

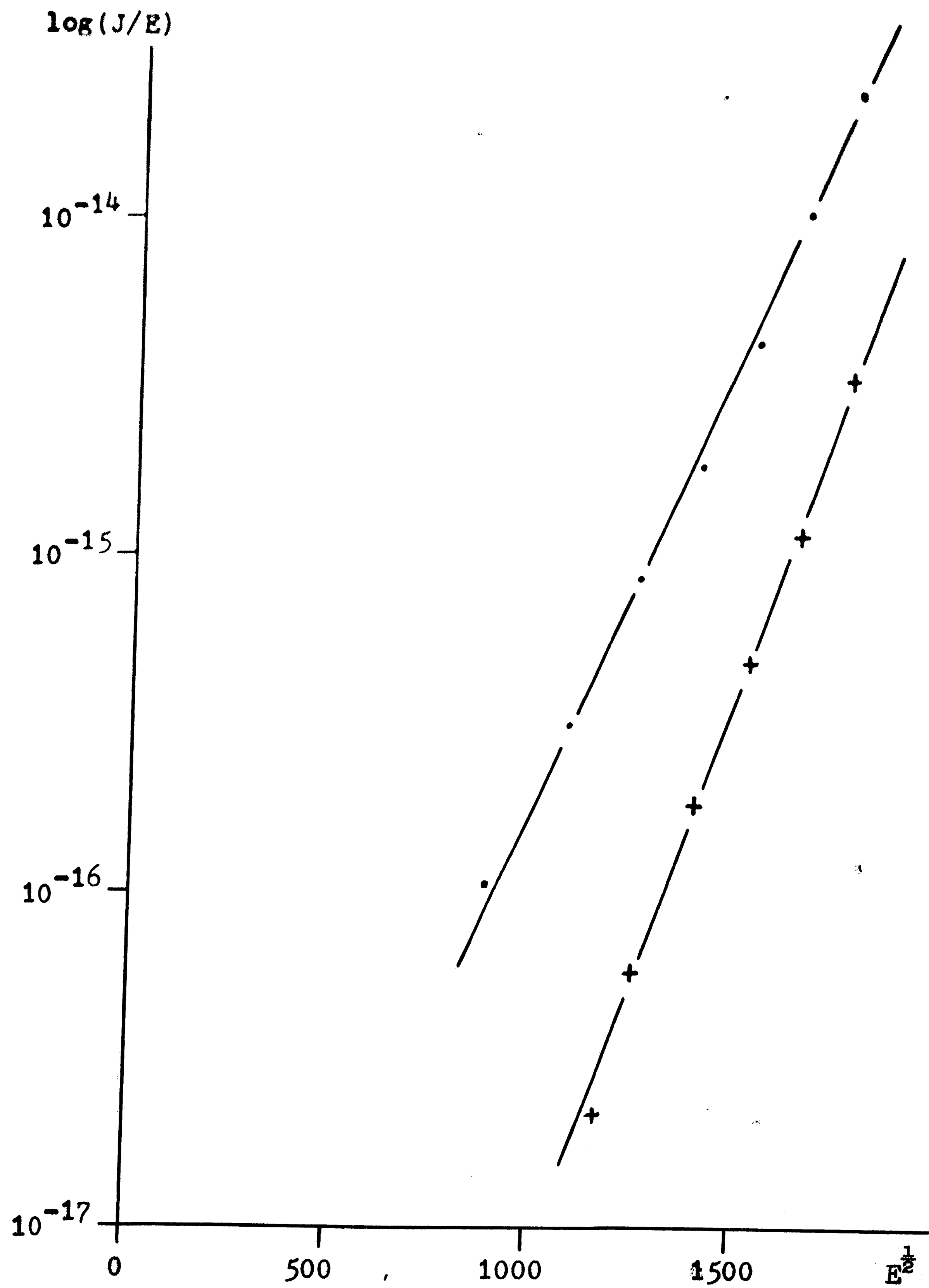


Figure 17. PEMA on n type substrate;

$X_0 = 1300 \text{ \AA}; A = 2 \times 10^{-3} \text{ cm}^2.$

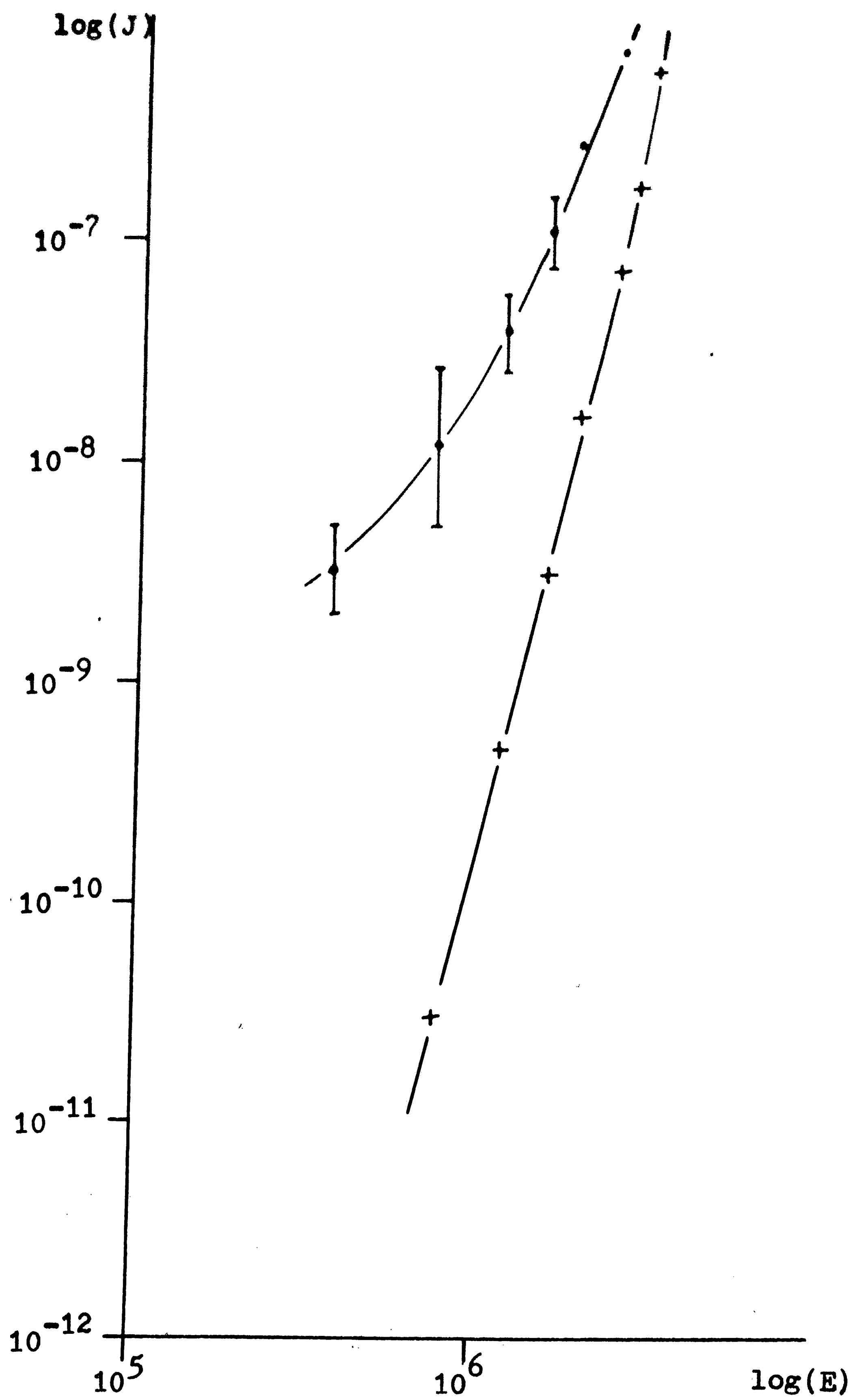


Figure 18. PEMA on p type substrate;

$X_0=1300\text{\AA}; A=2 \times 10^{-3} \text{cm}^2.$

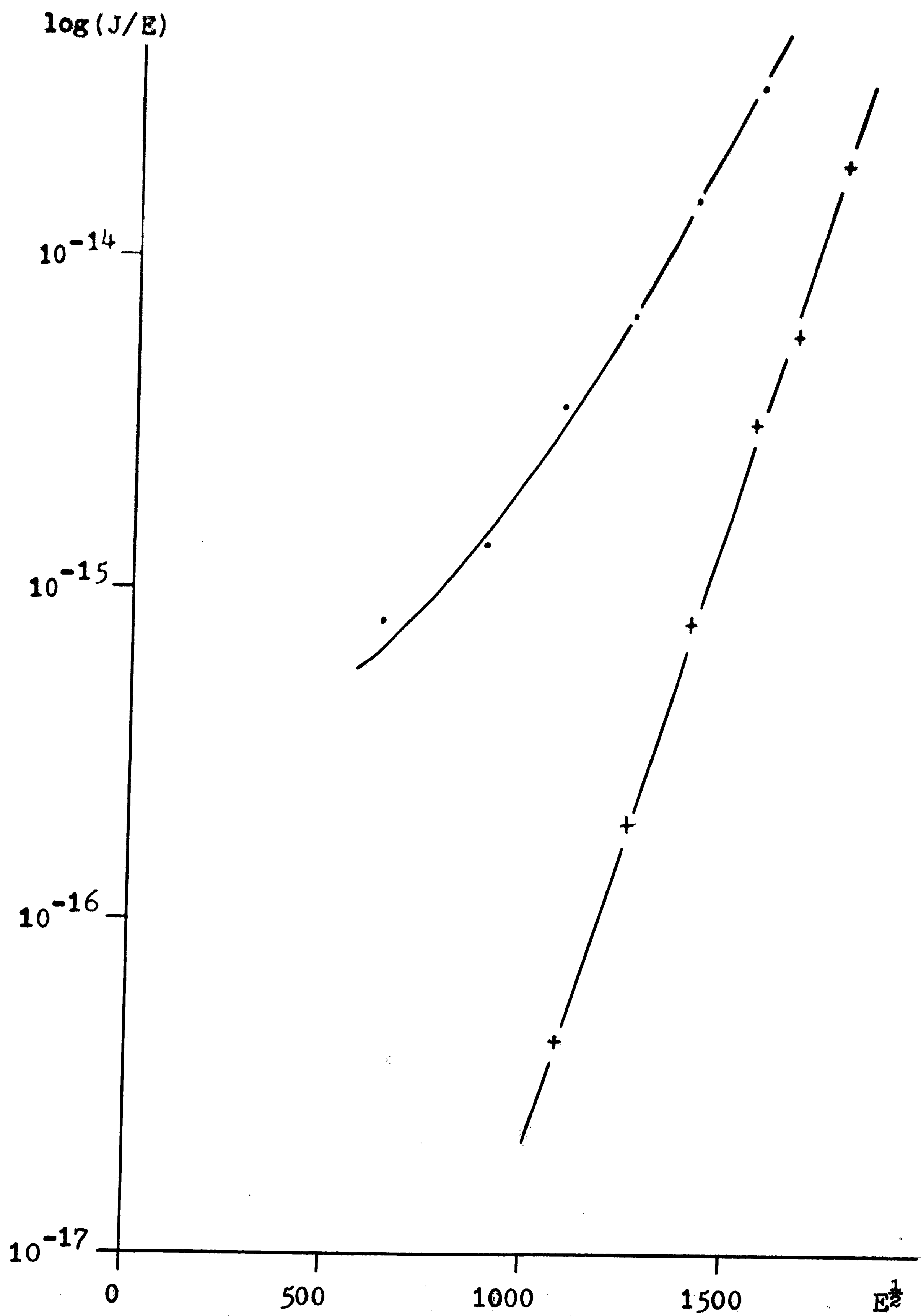


Figure 19. PEMA on p type substrate;
 $X_0=1300\text{\AA}$; $A=2 \times 10^{-3}\text{cm}^2$.

and negative voltage curves at low fields, especially in figure 18. The positive voltage space charge limited plots in figures 14, 15 and 18 have some regions of linearity with a slope of approximately 7. The negative voltage space charge limited plots seem to be non-linear which again suggests that the electrodes used have some effect on the current flow mechanism.

The difference in magnitude of the current flow illustrated in figures 14, 16 and 18 cannot be readily explained.

The field emission limited plots in figures 15, 17 and 19 are all linear except for the negative voltage curve in figure 15. Since linear field emission limited plots are expected for the Poole-Frenkel effect, this mechanism may apply for current flow in PEMA, with some effects due to the difference in the electrodes (i.e. the aluminum is used as the cathode in one case and silicon in the other case).

3.5 The Maleic Anhydride Copolymer

The data for the MA copolymer are summarized in figures 20-23. It is immediately obvious from a comparison of figures 20 and 22 that neither the polarity of the applied voltage, nor the conductivity type of the substrate, have any effect on the current flow in

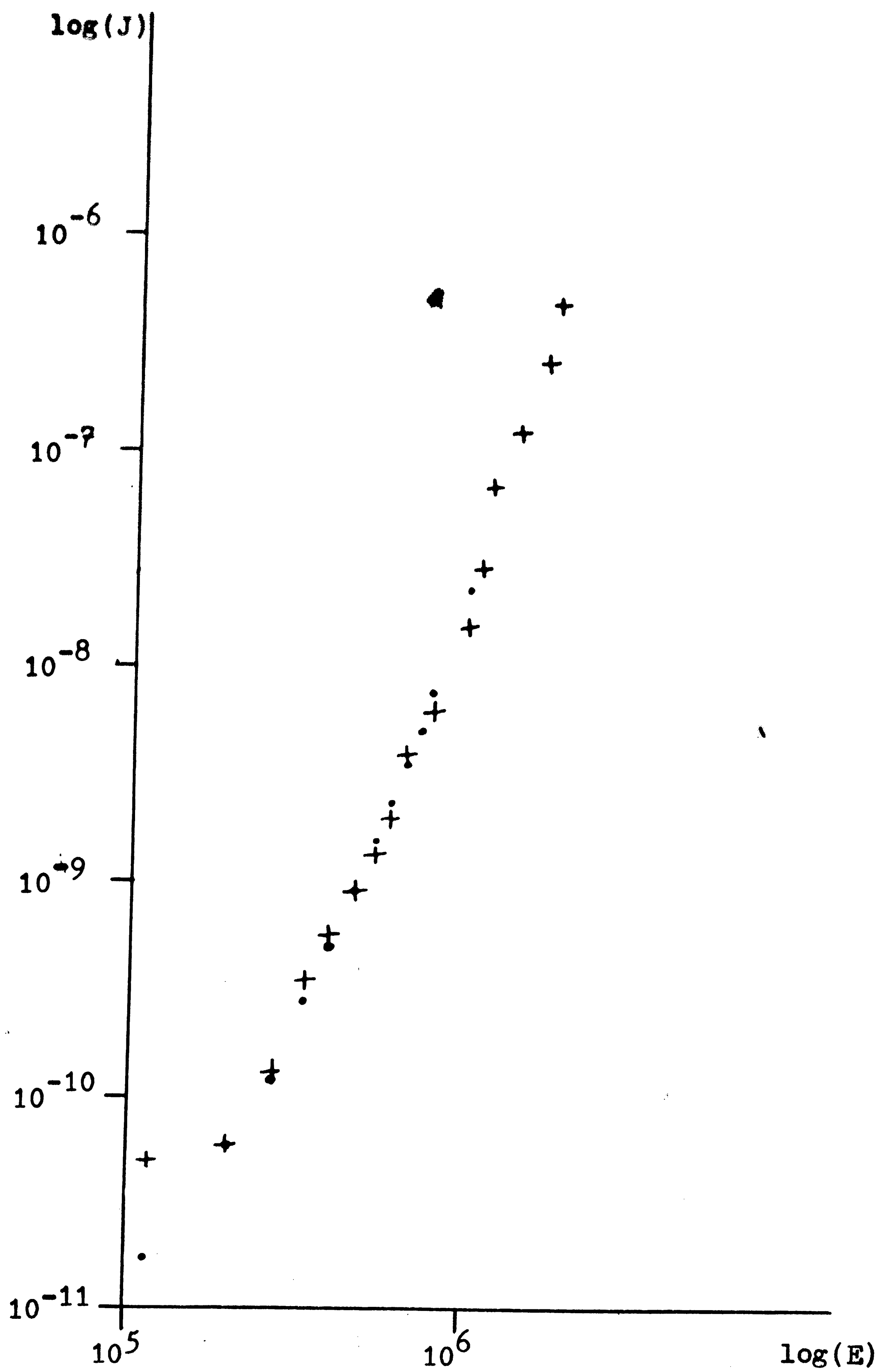


Figure 20. MA copolymer on p type substrate;

$X_0=1500\text{\AA}; A=2 \times 10^{-3}\text{cm}^2.$

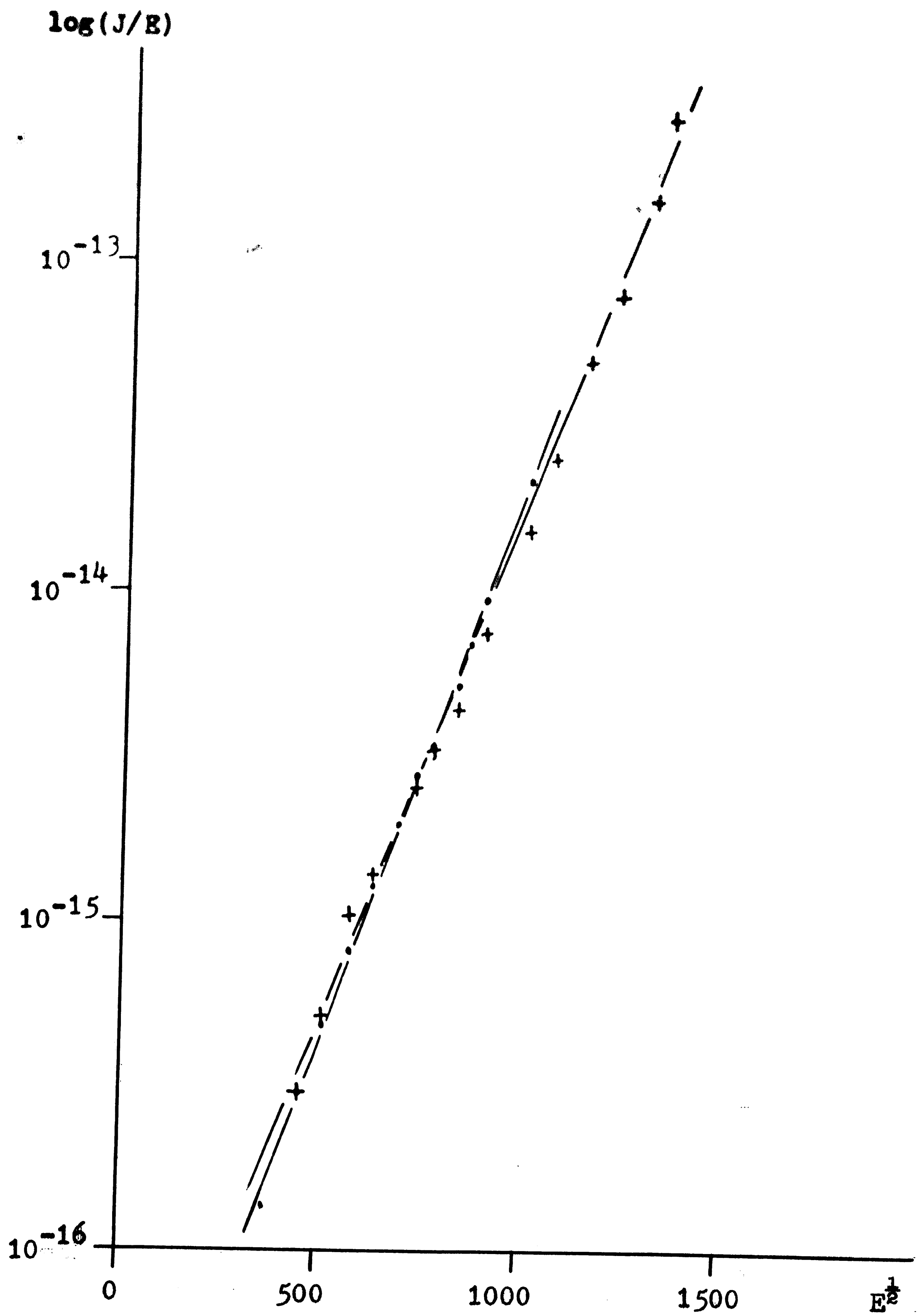


Figure 21. MA copolymer on p type substrate;

$X_0 = 1500 \text{ \AA}; A = 2 \times 10^{-3} \text{ cm}^2.$

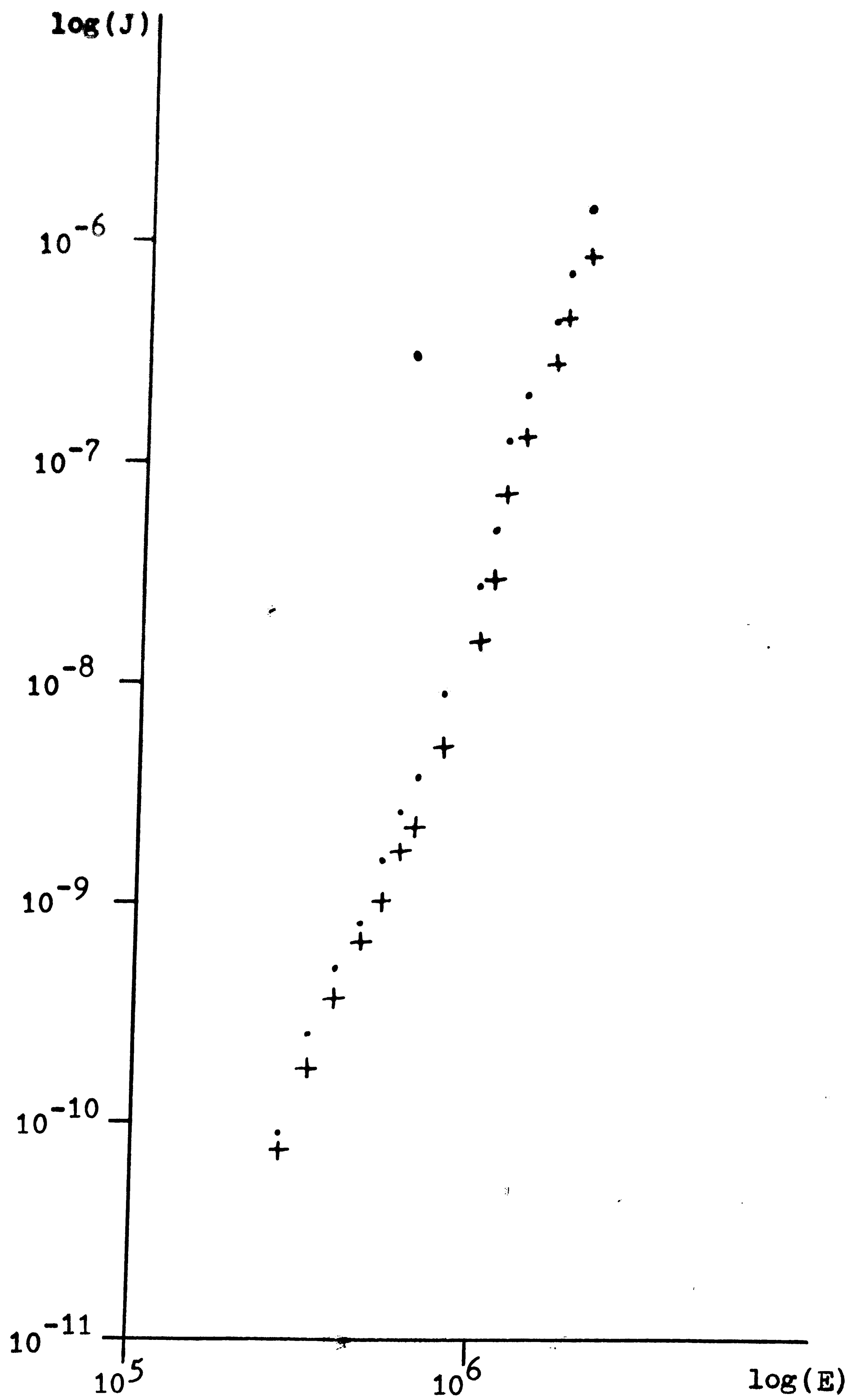


Figure 22. MA copolymer on n type substrate;

$X_0=1500\text{\AA}; A=2 \times 10^{-3}\text{cm}^2.$

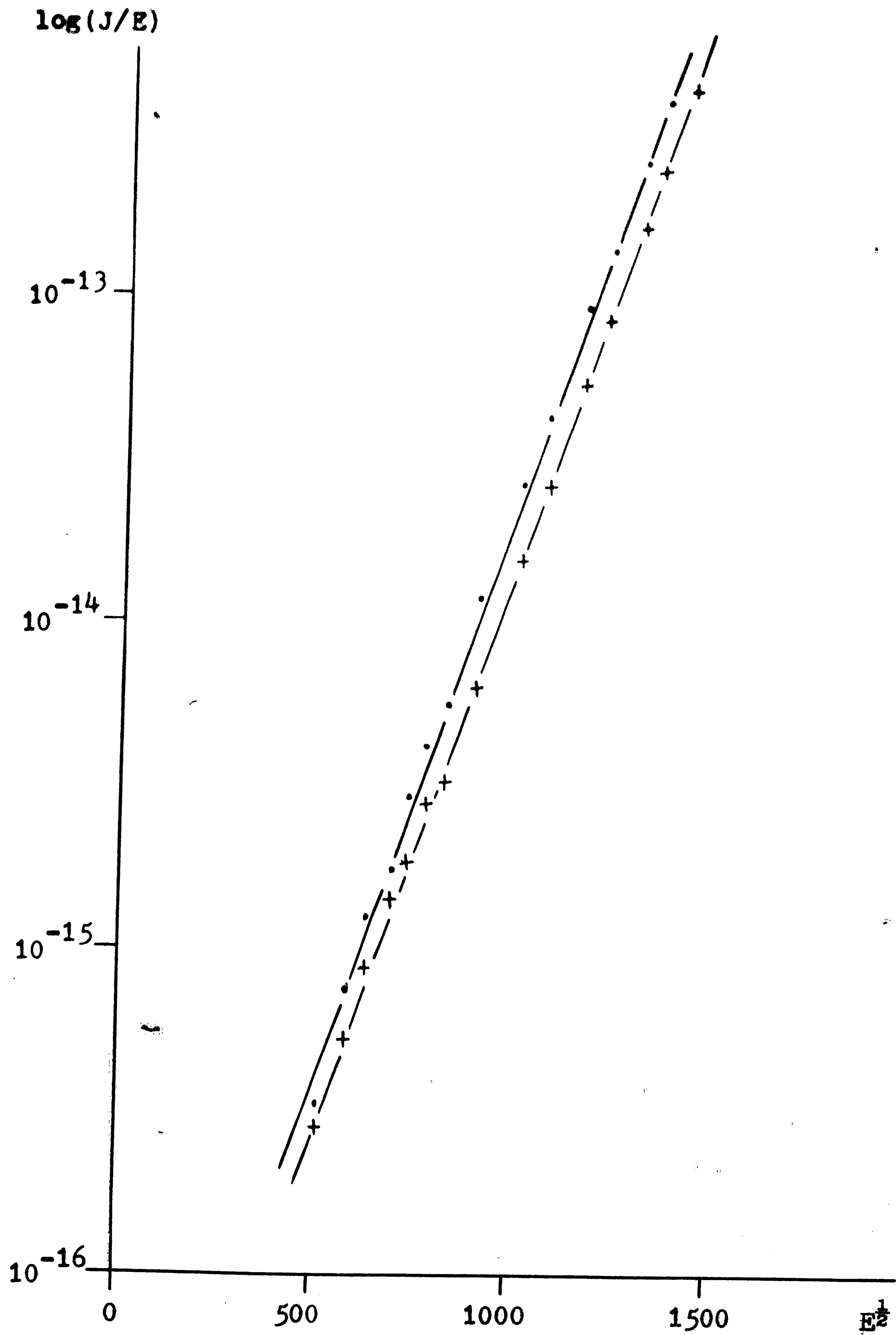


Figure 23. MA copolymer on n type substrate;

$X_0 = 1500 \text{ \AA}; A = 2 \times 10^{-3} \text{ cm}^2.$

this case.

The field emission limited current plots (figures 21 and 23) exhibit a linear relationship, whereas the space charge limited current plots (figures 20 and 22) do not. This suggests that the Poole-Frenkel effect may apply for the MA copolymer, however difficulty arises when comparing the theoretical and experimental values of the slope. If the Poole-Frenkel expression given by Sze is considered:

$$J \approx E \exp[-q(\phi_B - (qE/\pi\epsilon_i)^{1/2})/kT]$$

then the expression for the slope is, $m = (q/kT)(qE/\pi\epsilon_i)^{1/2}$ for a $\log(J/E)$ vs. $E^{1/2}$ plot. Using a value for ϵ_r of 2.7, results in a theoretical value of the slope, $m = 18.4 \times 10^{-3}$, but the experimental value of the slope from the $\log(J/E)$ vs. $E^{1/2}$ plot is 8.6×10^{-3} . These values disagree by a factor of 2, which indicates that the slope for Schottky emission, $m = (q/kT)(qE/4\pi\epsilon_f)^{1/2}$, would provide closer agreement. Jonscher [5] discusses this problem of finding agreement between data and the Poole-Frenkel expression or the Schottky emission expression. Hirose and Wada [14] required a value of $\epsilon_r = 12$ for silicon monoxide, which is unrealistically high, to obtain agreement with the Poole-Frenkel expression. Simmons [15] however, points out that the original form of the field emission limited expression is: $J \approx E \exp[-q(\phi_B - (qE/4\pi\epsilon_i)^{1/2})/kT]$.

and that this expression is the more proper one to use.

If this is true, then the theoretical value of the slope should be decreased by $\frac{1}{2}$, resulting in a value of 9.25×10^{-3} , which then agrees well with the experimental value of 8.6×10^{-3} . Thus it seems that the Poole-Frenkel effect, rather than the Schottky emission effect applies for current flow in the MA copolymer.

Part 4. SUMMARY

Some observations were found which were common to all four types of polymer films studied (polystyrene, CPE, PEMA and a MA copolymer); moisture and light had an effect on the current flow. Moisture on or within the polymer film increased the current flow by several orders of magnitude and changed the current flow mechanism as well. For positive applied voltages, ohmic current flow was observed for "wet" films of polystyrene. Light shining on the films increased the current flow approximately by a factor of 2, and may have changed the current flow mechanism as well.

The data for polystyrene was the most difficult to analyze since both linear space charge limited plots and linear field emission limited plots were obtained. It was also found that the type of electrode used for the cathode had an effect on the current flow. When silicon was used as the cathode, the current flow appeared to be space charge limited with an exponent of 2. However, when aluminum was used as the cathode, a linear space charge limited plot with a slope of approximately 5 was obtained. Since the material was the same in both cases, and thus had the same trap configuration, it is possible that the current flow may have been space charge limited in both cases, with the difference in electrodes producing a very

significant effect for polystyrene.

The data for CPE indicated that the current flow was space charge limited in this case, again with a difference in slope of the positive and negative voltage curves as discussed for polystyrene.

For PEMA, it was found that the current flow was most probably due to the Poole-Frenkel effect rather than space charge limitation, however, the electrodes used were found to affect the magnitude of the current flow.

The data for the MA copolymer was the clearest illustration of the Poole-Frenkel effect observed. It was found that the experimental slope agrees well with the theoretical slope calculated from the Poole-Frenkel field emission equation discussed by Simmons [15]. Furthermore no differences were observed for positive and negative applied voltages or between data for p type and n type substrates.

Although some fairly definite results were obtained (such as for the MA copolymer), other results are not entirely clear, thus it seems that more d.c. data is needed. Specifically, it will be important to obtain data from samples with various electrodes, data at various temperatures, and data from films of various thicknesses

of the same polymer. When this data becomes available, the precise mechanism of d.c. conductivity in polymers will become more clearly established.

BIBLIOGRAPHY

1. **Electronic Design**, 13, 54 (1973)
2. A. Bui, H. Carchano, and D. Sanchez, **Thin Solid Films**, 13, 207 (1972)
3. **Journal of the Electrochemical Society**, 119, 203C, 204C (1972)
4. M. E. Baird, **Journal of Polymer Science**, 8, 739 (1972)
5. A. K. Jonscher, **Thin Solid Films**, 1, 213 (1967)
6. F. E. Hartman, J. C. Blair and R. Bauer, **Journal of Applied Physics**, 37, 2468 (1966)
7. H. T. Mann, **Journal of Applied Physics**, 35, 2173, (1964)
8. N. M. Bashara and C.T. Doty, **Journal of Applied Physics**, 35, 3498 (1964)
9. M. Kryszewski and A. Szymanski, **Macromolecular Reviews**, 4, Part D, **Journal of Polymer Science**, 245 (1973)
10. Lampert and Mark, **Current Injection in Solids**, Academic Press, 45 (1970)
11. K. N. Mathes, **Encyclopedia of Polymer Science and Technology**, 5, 535 (1966)
12. S. M. Sze, **Physics of Semiconductor Devices**, Wiley-Interscience, 496 (1969)
13. K. N. Mathes, **Encyclopedia of Polymer Science and Technology**, 5, 546 (1966)
14. Hirose and Wada, **Japanese Journal of Applied Physics**, 4, 639 (1965)
15. J. G. Simmons, **Journal of Physics D: Applied Physics**, 4, 613 (1971)

VITA

Karl A. Sassaman, son of Karl H. and Mildred M. Sassaman, was born on August 23, 1949, in Bethlehem, Pennsylvania. He received a Bachelor of Science in Electrical Engineering degree from Lehigh University in June 1971. He married Rita G. Burke on August 19, 1972, and was commissioned as a 2 LT in the United States Army Reserve on May 27, 1973.